Circulation

ORIGINAL RESEARCH ARTICLE

Phosphoinositide 3-Kinase Gamma Inhibition Protects From Anthracycline Cardiotoxicity and Reduces Tumor Growth

BACKGROUND: Anthracyclines, such as doxorubicin (DOX), are potent anticancer agents for the treatment of solid tumors and hematologic malignancies. However, their clinical use is hampered by cardiotoxicity. This study sought to investigate the role of phosphoinositide 3-kinase γ (PI3Kγ) in DOX-induced cardiotoxicity and the potential cardioprotective and anticancer effects of PI3Kγ inhibition.

METHODS: Mice expressing a kinase-inactive PI3Kγ or receiving PI3Kγ-selective inhibitors were subjected to chronic DOX treatment. Cardiac function was analyzed by echocardiography, and DOX-mediated signaling was assessed in whole hearts or isolated cardiomyocytes. The dual cardioprotective and antitumor action of PI3Kγ inhibition was assessed in mouse mammary tumor models.

RESULTS: PI3Kγ kinase-dead mice showed preserved cardiac function after chronic low-dose DOX treatment and were protected against DOX-induced cardiotoxicity. The beneficial effects of PI3Kγ inhibition were causally linked to enhanced autophagic disposal of DOX-damaged mitochondria. Consistently, either pharmacological or genetic blockade of autophagy in vivo abrogated the resistance of PI3Kγ kinase-dead mice to DOX cardiotoxicity. Mechanistically, PI3Kγ was triggered in DOX-treated hearts, downstream of Toll-like receptor 9, by the mitochondrial DNA released by injured organelles and contained in autolysosomes. This autolysosomal PI3Kγ/Akt/mTOR/Ulk1 signaling provided maladaptive feedback inhibition of autophagy. PI3Kγ blockade in models of mammary gland tumors prevented DOX-induced cardiac dysfunction and concomitantly synergized with the antitumor action of DOX by unleashing anticancer immunity.

CONCLUSIONS: Blockade of PI3Kγ may provide a dual therapeutic advantage in cancer therapy by simultaneously preventing anthracyclines cardiotoxicity and reducing tumor growth.

Mingchuan Li, PhD
et al

Full author list is available on page 709

*Drs Hirsch and Ghigo contributed equally (see page 710).

Key Words: anthracyclines ■ autophagy ■ cardiotoxicity ■ immunosuppression ■ PI3Kγ

Sources of Funding, see page 710

https://www.ahajournals.org/journal/circ

Clinical Perspective

What Is New?

- The present study uncovers phosphoinositide 3-kinase γ as a major player of anthracyclines cardiotoxicity.
- The present study proposes phosphoinositide 3-kinase γ inhibition as an effective means to prevent the cardiac side effects of doxorubicin while boosting its anticancer action.

What Are the Clinical Implications?

- By virtue of its dual cardioprotective and anticancer action, phosphoinositide 3-kinase γ inhibition may ideally fit within chemotherapeutic regimens of both solid and hematologic tumors, including the highly prevalent form of breast cancer.
- Phosphoinositide 3-kinase γ inhibitors are currently in clinical trials, and future translational studies might help to validate our findings.

Anthracyclines such as doxorubicin are among the most potent and widely prescribed chemotherapeutics since the late 1960s and still remain cornerstones in cancer treatment in combination with new-generation targeted drugs. Their clinical use, however, is limited by cardiotoxicity, often requiring modification or even discontinuation of potentially successful anticancer regimens.[1] Cardiotoxicity occurs commonly within the first year after therapy completion, thus increasing morbidity and mortality among cancer survivors.[2]

Although clinical evaluation allows early detection of cardiotoxicity, effective prevention represents a still unmet clinical need. Small clinical trials have showed only modest effects of standard heart failure pharmacotherapy.[2] Dexrazoxane is the only cardioprotectant approved by the US Food and Drug Administration, but its use has been hindered by increased risk of developing secondary malignancies.[3,4] Ideally, optimal cardioprotective treatments should not only interfere with the primary mechanisms of cardiotoxicity but at least preserve or even enhance the antitumor efficacy of chemotherapy.

Phosphoinositide 3-kinase γ (PI3Kγ) has emerged as a crucial regulator of both cardiac function and tumorigenesis. Among class I PI3Ks, including PI3Kα, PI3Kβ, and PI3Kδ isoenzymes,[5] PI3Kγ plays a key maladaptive role in both heart disease and tumor growth.[10,11] In the heart, the catalytic subunit of the PI3Kγ holoenzyme (p110γ, the product of the *PIK3CG* gene), is upregulated under stress conditions and triggers adverse cardiac remodeling and, ultimately, heart failure.[6,7] PI3Kγ is also enriched in the tumor microenvironment and indirectly favors cancer growth by promoting macrophage trafficking and immunosuppressive polarization, which together prevent T cell-mediated tumor killing.[8,9] Accordingly, PI3Kγ inhibition protects against pressure overload-induced heart failure[6,7] and delays the progression of highly immunosuppressive tumors such as lung and pancreatic cancers.[8,10] Nonetheless, the role of PI3Kγ and the therapeutic potential of PI3Kγ inhibitors in anthracycline-mediated cardiomyopathy are so far unknown. Furthermore, how PI3Kγ-directed immunity interacts with anthracycline-based chemotherapy in the tumor remains unexplored.

Herein, we identify PI3Kγ as a key determinant of anthracycline cardiotoxicity, and we provide proof of concept that pharmacological inhibition of PI3Kγ is a unique means of preventing doxorubicin cardiotoxicity while boosting its anticancer efficacy. In cardiomyocytes, doxorubicin engages PI3Kγ signaling downstream of Toll-like receptor 9 (TLR9), converging on autophagy inhibition and maladaptive metabolic rewiring, which ultimately cause cardiomyocyte death and systolic dysfunction. Genetic or pharmacological blockade of PI3Kγ prevents anthracycline-induced heart disease and concomitantly synergizes with chemotherapy, delaying tumor growth and improving survival in xenograft and spontaneous mammary tumor models.

METHODS

The authors declare that all supporting data, analytic methods, and study materials are available within the article and its online supplementary files. Expanded methods can be found in the Methods section of the online-only Data Supplement. Key resources tables, including primary antibodies and quantitative *reverse transcription*-polymerase chain reaction primers, can be found in Tables I and II in the online-only Data Supplement.

Mice

Knockin mice expressing an inactive PI3Kγ holoenzyme (kinase dead [KD]) were generated by inserting a point mutation in the *Pik3cg* gene encoding the p110γ catalytic subunit as previously described.[11] For studies on spontaneous tumors, BALB/c mice overexpressing the activated form of the Neu oncogene (BALB/c rHER-2/NeuT) in the mammary gland were used.[12] Authorities approved all animal experiments.

In Vivo Treatments

To mimic human therapeutic regimens, a cumulative dose of 12 mg/kg of doxorubicin (DOX) was administered via 3 weekly IP injections (4 mg/kg on days 0, 7, and 14).[13] Survival was monitored daily. To investigate Akt/mTOR/Ulk1 signaling, wild-type (WT) and KD mice received a single IP injection of 4 mg/kg DOX alone or in combination with 100 μg of ODN2088 (TLR9 antagonist) for 3 days.

To study the autophagic flux in vivo, mice were treated IP with 10 mg/kg bafilomycin A1 (BafA1) or vehicle 1 hour

before a single injection of 4 mg/kg DOX. Mice were euthanized 6 hours after DOX.

To inhibit autophagy in vivo, PI3Kγ KD mice were treated with DOX or saline, followed by daily IP injections of 60 mg/kg of hydroxychloroquine or 0.3 mg/kg of BafA1 or saline for 4 weeks. Cardiomyocyte-restricted, genetic inhibition of autophagy was performed by intravenous injection of either AAV9-GFP-U6-ATG7-small hairpin RNA or AAV9-GFP-U6-scrmb-small hairpin RNA.

Echocardiography

Cardiac function was evaluated in mice anesthetized with 1% isoflurane using a Vevo2100 High Resolution Imaging System (Visual Sonics Inc). Echocardiographic parameters were measured under the long-axis M-mode when heart rate was ≈450 bpm.

Tumor Studies

Mice were subcutaneously injected with 1×10^5 4T1 or TUBO cells. One week after cell injection, mice were treated with DOX or saline. Tumor size was measured twice per week for 4 weeks. PI3Kγ was inhibited pharmacologically by using IPI145[14] and AS605240.[15]

Isolation of Neonatal Mouse Ventricular Myocytes

Neonatal mouse cardiomyocytes (NMVMs) were isolated as previously described.[16] Briefly, hearts from 1- to 3-day-old pups were minced and predigested with 0.5 mg/mL trypsin overnight, followed by 3 to 4 digestions with 330 U/mL collagenase type II. Isolated cells were centrifuged at 800 rpm to separate nonmyocardial cells; resuspended in DMEM/M199 (3:1) containing 10% horse serum, 5% fetal bovine serum, and 5 mM penicillin/streptomycin; and preplated twice to further reduce fibroblast contamination. 0.3 to 1×10^6 cardiomyocytes per well were finally plated in gelatin (0.2%)/fibronectin (10 μg/mL)-coated plates. Expanded methods can be found in the online-only Data Supplement.

In Vitro Treatments

Twenty-four hours before stimulation, NMVMs were cultured in serum-free DMEM/M199 (3:1) and H9c2 cells in DMEM supplemented with 0.5% fetal bovine serum. Cells were then treated with 1 μmol/L DOX for the indicated times, alone or in combination with AS605240 (0.5 μmol/L, 1-hour pretreatment) or with the TLR9 antagonist ODN2088 (0.2 μmol/L, 5-hour pretreatment) as described previously.[17] Alternatively, NMVMs and H9c2 cells were stimulated with the TLR9 agonist ODN1826 (0.2 μmol/L, 1 hour) with or without AS605240 pretreatment. At the end of treatment, cells were processed as described previously.[6]

Flow Cytometry Staining and Analysis

Single-cell suspensions from mouse tumor samples (1×10^6 cells) were incubated with the blocking reagent anti-CD16/CD32, followed by incubation with fluorophore-labeled antibodies. For staining of surface markers, the following primary antibodies were used: Gr1 Ly6G/Ly6C, F4/80, CD11b, and MHC class II. For CD206 staining, formalin-fixed cells were incubated with a fluorophore-labeled antibody. Cells were acquired with the AccuriC6 and analyzed with FlowJo x7.5.

Histological and Immunohistochemical Analysis

mtDNA, TLR9, PI3Kγ, and LAMP2 colocalization was assessed in NMVMs stimulated with either ODN1826 or DOX for 1 hour. Standard protocols were used for immunofluorescence staining. For ex vivo analyses, hearts from WT and KD mice treated with DOX or saline were processed for histological and immunofluorescence analysis.[18]

Human heart samples were collected from a 21-year-old woman diagnosed with Ewing sarcoma and subjected to triple therapy with adriamycin, cyclophosphamide, and vincristine. The patient manifested heart failure symptoms 5 years after chemotherapy and underwent heart transplantation 10 years after the diagnosis of chemotherapy-induced cardiomyopathy (ejection fraction: 40%). Samples were archived at the Institute of Pathological Anatomy of the University of Padova. Samples were anonymous to the investigators and used in accordance with the directives of authorities. Formalin-fixed, paraffin-embedded human heart samples were processed for immunofluorescence study.[19]

Statistical Analysis

Prism software (GraphPad software Inc) was used for statistical analysis. *P* values were calculated with 1-way analysis of variance (ANOVA), 2-way ANOVA, 2-way repeated-measures ANOVA, followed by Bonferroni post hoc test or Student's *t* test as appropriate. Log-rank test was used for survival analysis. Data are presented as mean±SEM, and $P<0.05$ was considered statistically significant.

RESULTS

Genetic Inhibition of PI3Kγ Protects Against DOX Cardiotoxicity

To explore the role of PI3Kγ in anthracycline-induced cardiotoxicity, knockin mice expressing a kinase-inactive PI3Kγ (PI3Kγ KD) and WT controls were subjected to a low-dose DOX treatment[13] (Figure IA in the online-only Data Supplement). The treatment was well tolerated by both WT and KD mice, as evidenced by preserved food intake and locomotor activity (Figure IB and IC in the online-only Data Supplement). In line with clinical evidence of weight loss in DOX-treated patients,[20,21] DOX induced a 10% decrease in body weight in both genotypes, without significantly affecting survival (Figure ID and IE in the online-only Data Supplement). Echocardiographic assessment 6 weeks after the first DOX administration revealed a significant reduction of cardiac contractility in WT mice (Figure 1A and Table III in the online-only Data Supplement), which was accompanied by upregulation of cardiac injury markers such as

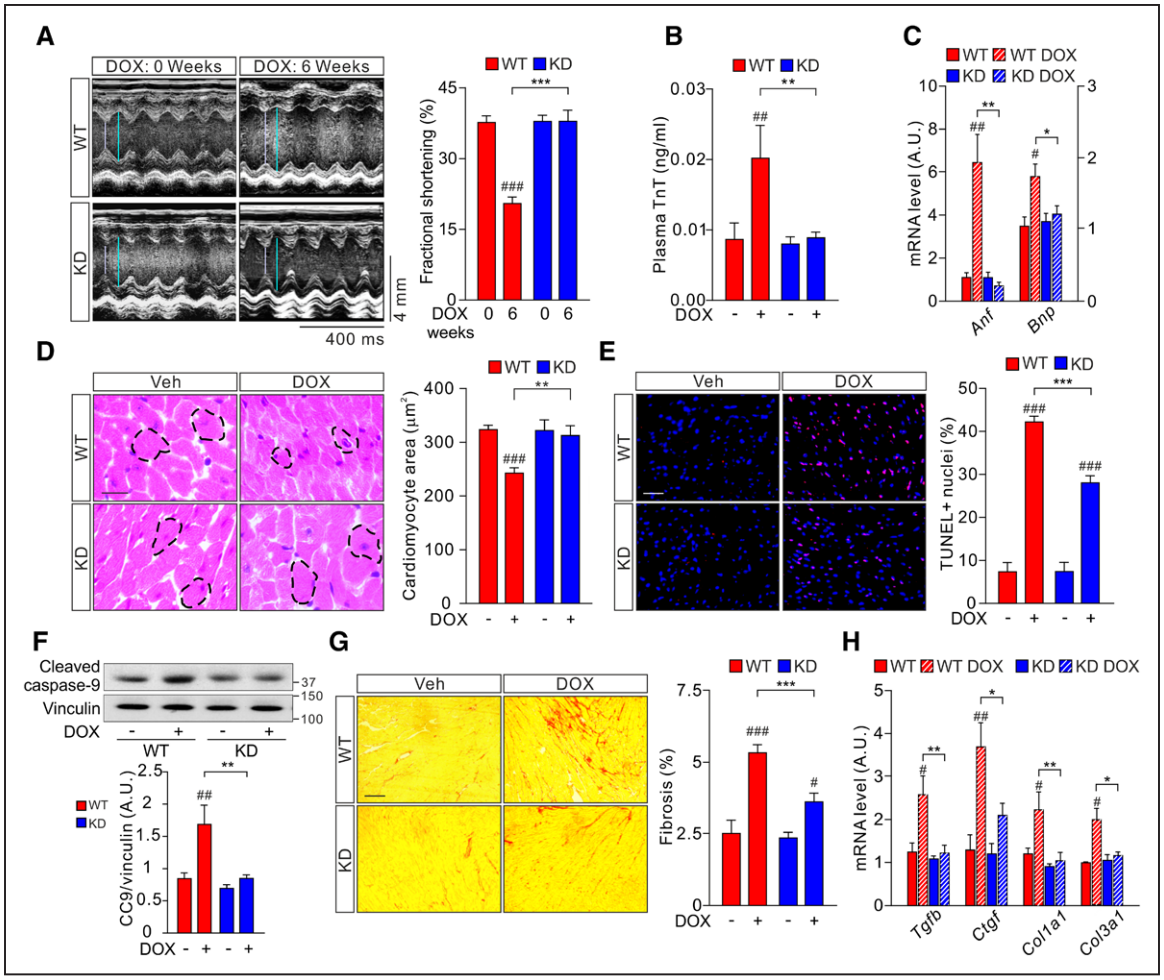

Figure 1. Genetic inhibition of PI3Kγ protects against DOX-induced cardiotoxicity.
WT and KD mice were treated with a cumulative dose of 12 mg/kg doxorubicin (DOX) or saline via 3 weekly injections (4 mg/kg on days 0, 7, and 14). **A,** Representative M-mode echocardiographic images (left) and fractional shortening (right) of WT (n=9) and KD (n=9) hearts before treatment and 6 weeks after the first DOX injection. White and cyan lines indicate left ventricular end-diastolic diameter (LVEDD) and left ventricular end-systolic diameter (LVESD), respectively. Scale bars, 400 ms, 4 mm. DOX 0 versus 6 weeks: ###*P*<0.001 and WT versus KD, ***P<0.001 by 2-way repeated-measures analysis of variance with Bonferroni post hoc test. **B,** Plasma troponin T (TnT) level in WT and KD mice 3 days after the first dose of DOX or saline. **C,** Relative quantification of *Anf* and *Bnp* mRNA levels in WT and KD whole hearts at 6 weeks after the first dose of DOX or saline. **D,** Representative images of H&E staining and relative quantification of cardiomyocyte area in heart sections from mice treated as in (**C**). Scale bar, 20 μm. **E,** Representative images of TUNEL staining (left) and quantification of TUNEL positive nuclei per field (right) in WT and KD in heart sections from mice treated as in (**C**). Scale bar, 30 μm. **F,** Immunoblot (upper) and relative quantification (lower) of cleaved-caspase 9 in whole hearts from WT and KD mice treated as in (**C**). **G,** Representative images of PicroSirius Red staining (left) and relative quantification of collagen deposition (right) in heart sections from animals treated as in (**C**). Scale bar, 50 μm. **H,** Relative quantification of mRNA levels of profibrotic genes (*Tgfb*, *Ctgf*, *Col1a1*, and *Col3a1*) in whole hearts from animals treated as in (**C**). For each panel in (**B** through **H**): n=5 to 7 animals/group, DOX (+) versus saline (–): #*P*<0.05, ##*P*<0.01, and ###*P*<0.001 and WT versus KD: *P<0.05, **P<0.01, and ***P<0.001 by 2-way analysis of variance with Bonferroni post hoc test. Values represent mean±SEM. Anf indicates atrial natriuretic factor; Bnp, brain natriuretic peptide; Col1a1, collagen type I alpha-1; Col3a1, collagen type III alpha-1; Ctgf, connective tissue growth factor; DOX, doxorubicin; KD, kinase-dead; LVEDD, left ventricular end-diastolic diameter; LVESD, left ventricular end-systolic diameter; PI3Kγ, phosphoinositide 3-kinase γ; Tgfb, transforming growth factor beta; TnT, troponin T; TUNEL, terminal deoxynucleotidyl transferase dUTP nick end labeling; and WT, wild-type.

plasma concentrations of troponin T (Figure 1B) and myocardial *Anf* and *Bnp* mRNA levels (Figure 1C). The absence of lung and liver congestion in these mice (Table IV in the online-only Data Supplement) excluded the development of overt heart failure and indicated the establishment of a subclinical myocardial dysfunction, reminiscent of that observed clinically in chronic DOX cardiomyopathy. Conversely, left ventricular systolic function, plasma troponin T, and *Anf* and *Bnp* mRNA levels were all unchanged in DOX-treated KD mice

(Figure 1A through 1C and Table III in the online-only Data Supplement), highlighting the protective effects of PI3Kγ inhibition against DOX-induced cardiac injury.

Cardiac wasting, apoptosis, and fibrosis are key hallmarks of anthracycline-related cardiotoxicity.[22] In keeping with preserved cardiac contractility, KD mice showed normal cardiac mass and cardiomyocyte size after DOX (Figure 1D and Table IV in the online-only Data Supplement). Furthermore, TUNEL and cleaved caspase-9 assays revealed that, after DOX treatment, apoptosis was significantly lower in KD than in WT hearts (Figure 1E and 1F). Myocardial collagen deposition was significantly less abundant in DOX-treated KD than in WT hearts, as evidenced by reduced PicroSirius Red staining (Figure 1G) and by weaker expression of profibrotic genes such as *Tgfb*, *Ctgf*, *Col1a1*, and *Col3a1* (Figure 1H).

Altogether, these findings demonstrate that PI3Kγ inhibition protects against DOX-induced myocardial damage and dysfunction.

PI3Kγ Inhibition Promotes Mitochondrial Autophagy

Although PI3Kγ can contribute to maladaptive cardiac remodeling by driving inflammation,[7] analysis of inflammatory responses after DOX showed no significant leukocyte recruitment to the myocardium of either WT or KD mice (Figure II in the online-only Data Supplement). This excluded the involvement of leukocyte PI3Kγ in DOX-induced cardiac remodeling.

Conversely, the PI3K pathway is a master regulator of autophagy,[23] and dysregulation of autophagy in the myocardium is implicated in cardiovascular diseases, including DOX cardiotoxicity.[24–27] The possible link between myocardial PI3Kγ signaling and autophagy was thus investigated in DOX-treated animals. The levels of LC3-II, a hallmark of autophagosome formation, were slightly but significantly increased in WT hearts at 3 days after the first injection of DOX (Figure 2A). In contrast, LC3-II accumulation was significantly higher in

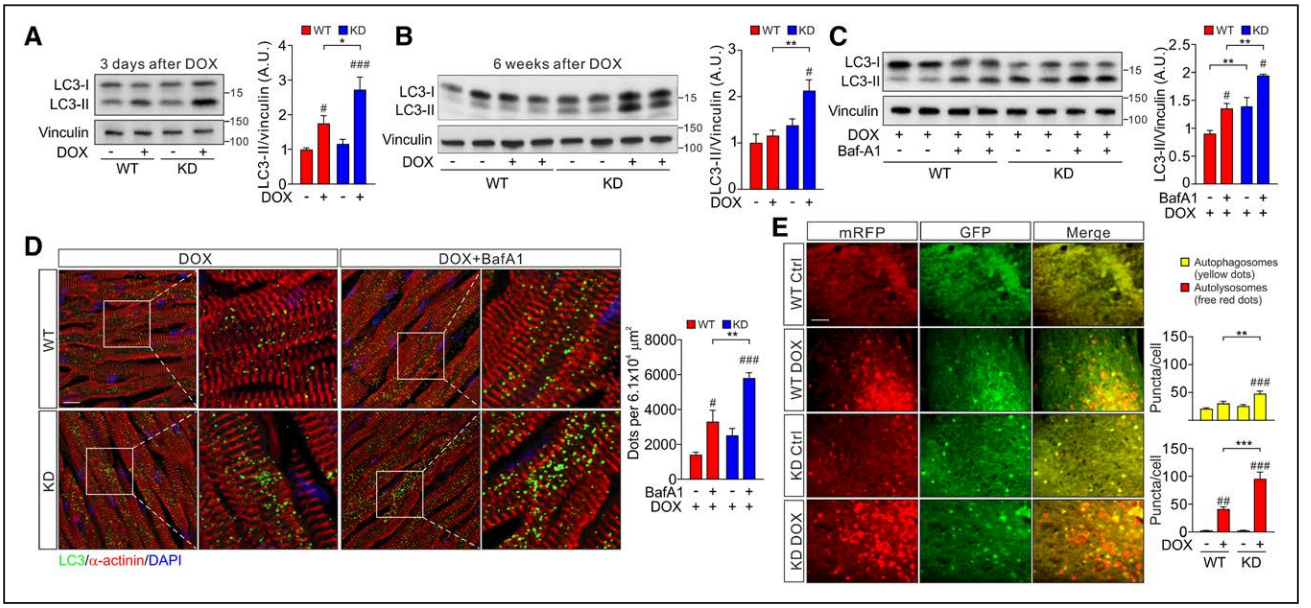

Figure 2. PI3Kγ inhibition promotes cardiac autophagy.
A and **B,** Representative immunoblot (left) and relative quantification (right) of the autophagic marker LC3 in WT and KD hearts 3 days (**A**) and 6 weeks (**B**) after DOX. n=5 to 8 animals/group. **A** through **B**, DOX (+) versus saline (–): #*P*<0.05 and ###*P*<0.001 and WT versus KD: **P*<0.05 and ***P*<0.01 by 2-way analysis of variance with Bonferroni post hoc test. **C,** Autophagic flux analysis in WT and KD mice pretreated with bafilomycin A1 (BafA1, 10 mg/kg) 1 hour before a single DOX injection (4 mg/kg) for 6 hours. Representative immunoblots (left) and relative quantification (right) are shown. **D,** Immunofluorescence staining (left) and relative quantification (right) of LC3 puncta in heart sections from animals treated as in (**C**). Scale bar, 10 μm. **C** through **D**, n=5 to 6 animals/group, DOX+saline versus DOX+BafA1: #*P*<0.05 and ###*P*<0.001 and WT versus KD: ***P*<0.01 by 2-way analysis of variance with Bonferroni post hoc test. **E,** WT and KD neonatal mouse ventricular myocytes (NMVMs) were infected with an adenovirus encoding the tandem fluorescent mRFP-GFP-LC3 probe before treatment with DOX (1 μM, 16 hours). Representative pictures (left, magnification of Figure III in the online-only Data Supplement) and relative quantification (right) of autophagosomes (yellow dots) and autolysosomes (red free dots) are shown. Scale bar, 2 μm. n≥4 independent experiments. DOX versus vehicle: ##*P*<0.01 and ###*P*<0.001 and WT versus KD: ***P*<0.01 and ****P*<0.001 by 2-way analysis of variance with Bonferroni post hoc test. Values represent mean±SEM. BafA1 indicates bafilomycin A1; DOX, doxorubicin; GFP, green fluorescent protein; KD, kinase-dead; LC3, microtubule-associated protein 1A/1B-light chain 3; mRFP, monomeric red fluorescent protein; NMVMs, neonatal mouse ventricular myocytes; PI3Kγ, phosphoinositide 3-kinase γ; and WT, wild-type.

KD than in WT hearts, starting from this time point (Figure 2A) and up to the end of the treatment (Figure 2B), thus indicating that PI3Kγ acts as a negative regulator of autophagy. This result was further demonstrated in primary NMVMs expressing YFP-LC3, where LC3-puncta (autophagosomes) elicited by DOX were significantly more abundant in KD than in WT cells (Figure IIIA in the online-only Data Supplement).

To assess whether LC3-II accumulation in KD hearts resulted from enhanced autophagosome formation or impaired autophagosome-lysosome fusion, autophagic flux was studied after blocking autophagosome-lysosome fusion with BafA1. BafA1 further increased LC3-II levels (Figure 2C) and LC3 puncta density (Figure 2D) in DOX-treated KD hearts, thus revealing that loss of PI3Kγ catalytic function enhances activation of the autophagic flux. These findings were confirmed in primary NMVMs expressing the mRFP-GFP-LC3 probe, which allows the concomitant detection of autophagosomes (yellow dots) and autolysosomes (free red dots) in living cells.[28] Both yellow and red puncta were significantly more abundant in KD than in WT NMVMs (Figure 2E and Figure IIIB in the online-only Data Supplement), confirming an accelerated autophagic flux in KD cardiomyocytes exposed to DOX. Pretreatment with BafA1 prevented the formation of autolysosomes in both groups and further proved enhanced formation of autophagosomes in KD cells compared with WT controls (Figure IIIC in the online-only Data Supplement). Thus, PI3Kγ acts as a negative regulator of autophagy in DOX-treated hearts.

Alteration of the autophagic flux in cardiomyocytes can reduce their ability to eliminate DOX-damaged organelles such as mitochondria.[29] Electron microscopy studies revealed the presence of autophagic vacuoles containing damaged mitochondria in DOX-treated WT hearts (Figure 3A), indicating the activation of mitochondrial autophagy. In keeping with an enhanced autophagic flux (Figure 2C through 2E), these structures were more abundant in KD hearts than in WT controls (Figure 3A). Immunofluorescence studies showing the colocalization of mitochondrial DNA (mtDNA) with the autophagosome marker LC3 (Figure 3B), and LC3-II immunoblot in mitochondria-enriched fractions (Figure IVA in the online-only Data Supplement) both confirmed that mitochondrial autophagy was significantly more active in KD than in WT hearts after DOX.

Enhanced elimination of injured organelles led to preserved mitochondrial respiration in NMVMs exposed to DOX concomitantly to the PI3Kγ inhibitor AS605240 (Figure IVB in the online-only Data Supplement). Instead, in cells treated with DOX alone, the bioenergetic efficiency of mitochondria (P/O ratio) was significantly reduced and triggered a compensatory metabolic switch from fatty acid oxidation to glycolysis, as indicated by increased activity of major glycolytic enzymes, higher lactate dehydrogenase activity, and lactate production (Figure IVB in the online-only Data Supplement). PI3Kγ was not expressed in the mitochondria (Figure IVC in the online-only Data Supplement), thus excluding the involvement of PI3Kγ in intrinsic mitochondrial regulation and suggesting that PI3Kγ inhibition preserves mitochondrial metabolism indirectly by favoring autophagic disposal of damaged organelles.

DOX Activates an Autolysosomal Toll-Like Receptor 9 /PI3Kγ Pathway Promoting Feedback Inhibition of Autophagy

Given that damaged mitochondria within autolysosomes can trigger Toll-like receptor 9 (TLR9),[17] and TLRs can signal through PI3Kγ activation,[30] the ability of mtDNA from DOX-injured mitochondria to engage TLR9 and, in turn, PI3Kγ signaling was investigated. Immunofluorescence assays revealed that mtDNA colocalized with both TLR9 and PI3Kγ in NMVMs exposed to DOX (Figure 4A), in line with the localization of PI3Kγ in endosomes[31] as well as with the enrichment of these 3 moieties in similar endocytic compartments. In resting cells, TLR9 mainly resides in the endoplasmic reticulum but translocates to lysosomes on induction of autophagy.[32] Consistently, immunofluorescence (Figure 4B) and coimmunoprecipitation studies (Figure 4C) showed that colocalization of TLR9 with PI3Kγ can only be detected in cells challenged with the TLR9 activator ODN1826, a CpG-rich oligonucleotide similar to mtDNA, but not in untreated controls. In NMVMs treated with ODN1826, both TLR9 and PI3Kγ were found in LAMP2-positive compartments (autolysosomes) (Figure 4D), thus indicating that the TLR9/PI3Kγ signaling complex assembles on these organelles.

Next, PI3Kγ pathway activation by the DOX/mitochondrial damage/mitochondrial autophagy/mtDNA/TLR9 cascade was investigated in H9c2 cardiac-like cells, primary NMVMs, and whole hearts. In H9c2, DOX increased the phosphorylation of the PI3K downstream target Akt as early as 30 minutes and until 2 hours after treatment, and the PI3Kγ selective inhibitor AS605240 completely prevented DOX-dependent Akt activation (Figure VA in the online-only Data Supplement). Similarly, Akt phosphorylation was upregulated 2-fold in WT but not in KD primary NMVMs exposed to DOX (Figure VB in the online-only Data Supplement). It is notable that DOX-dependent PI3Kγ/Akt activation occurred downstream of TLR9 because the TLR9 antagonist ODN2088 prevented Akt phosphorylation in both NMVMs (Figure 5A) and H9c2 (Figure VIA in the online-only Data Supplement), mimicking the ef-

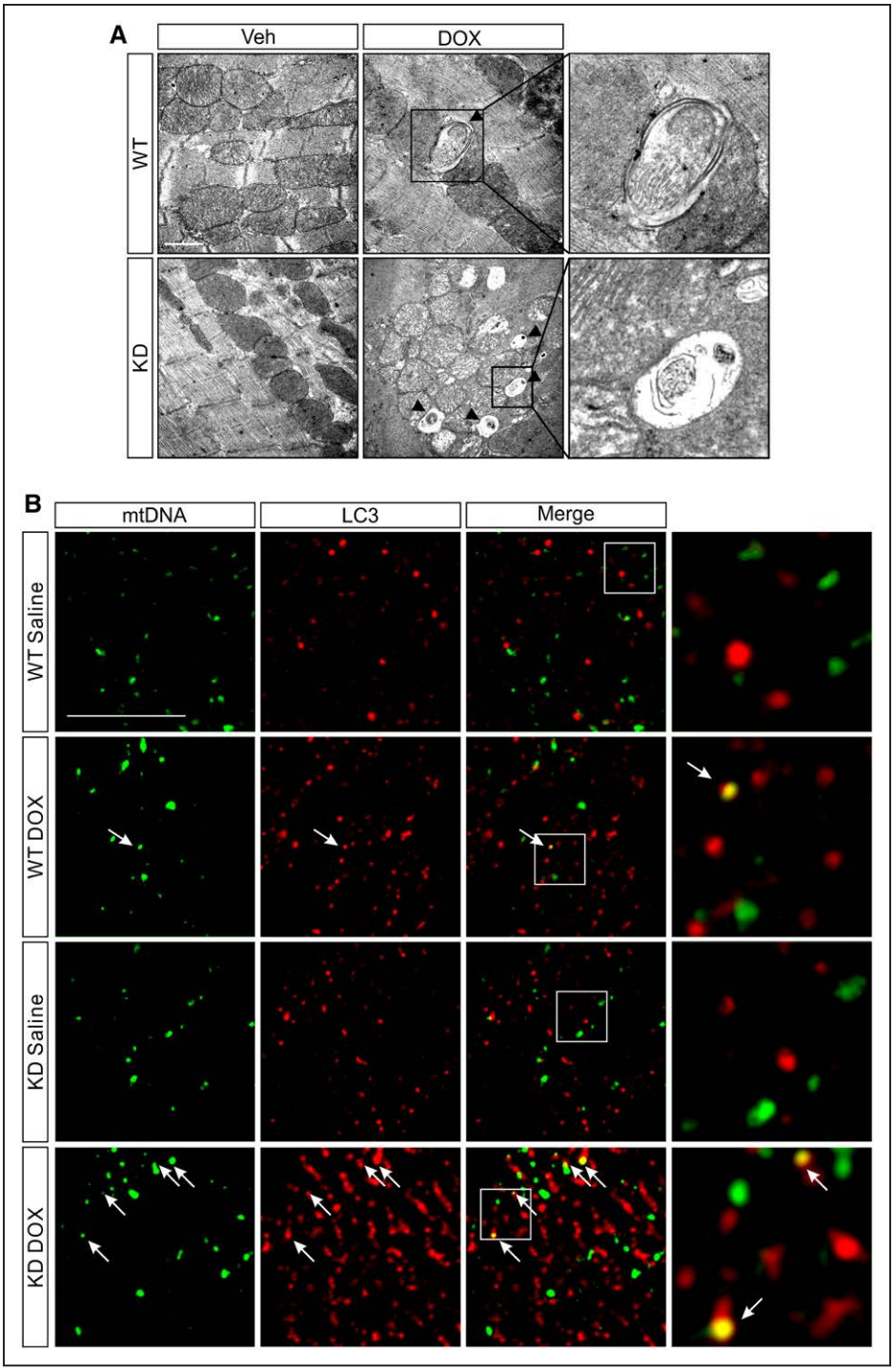

Figure 3. PI3Kγ inhibition promotes autophagic clearance of damaged mitochondria.
A, Transmission electron micrographs of WT and KD hearts 3 days after a single injection of doxorubicin (DOX, 4 mg/kg). Scale bar, 1 μm. Black arrows and magnification insets show autophagic vacuoles containing damaged mitochondria. **B,** Double staining of mitochondrial DNA (mtDNA) with PicoGreen (green) and autophagosomes with an anti-LC3 antibody (red) in heart sections from WT and KD mice treated as in (**A**). In merged images and magnification insets, arrows indicate double positive deposits (yellow dots). Scale bar, 10 μm. In (**A**) and (**B**), representative pictures from n=3 experiments are shown. DOX indicates doxorubicin; KD, kinase-dead; LC3, microtubule-associated protein 1A/1B-light chain 3; mtDNA, mitochondrial DNA; PI3Kγ, phosphoinositide 3-kinase γ; Veh, vehicle; and WT, wild-type.

fects of PI3Kγ inhibition (WT NMVMs treated with AS605240 and KD NMVMs in Figure 5A; AS605240-treated H9c2 cells in Figure VIA in the online-only Data Supplement). In further support of the activation of a TLR9/PI3Kγ/Akt signaling on induction of mitochondrial autophagy, the mtDNA-like oligonucleotide and

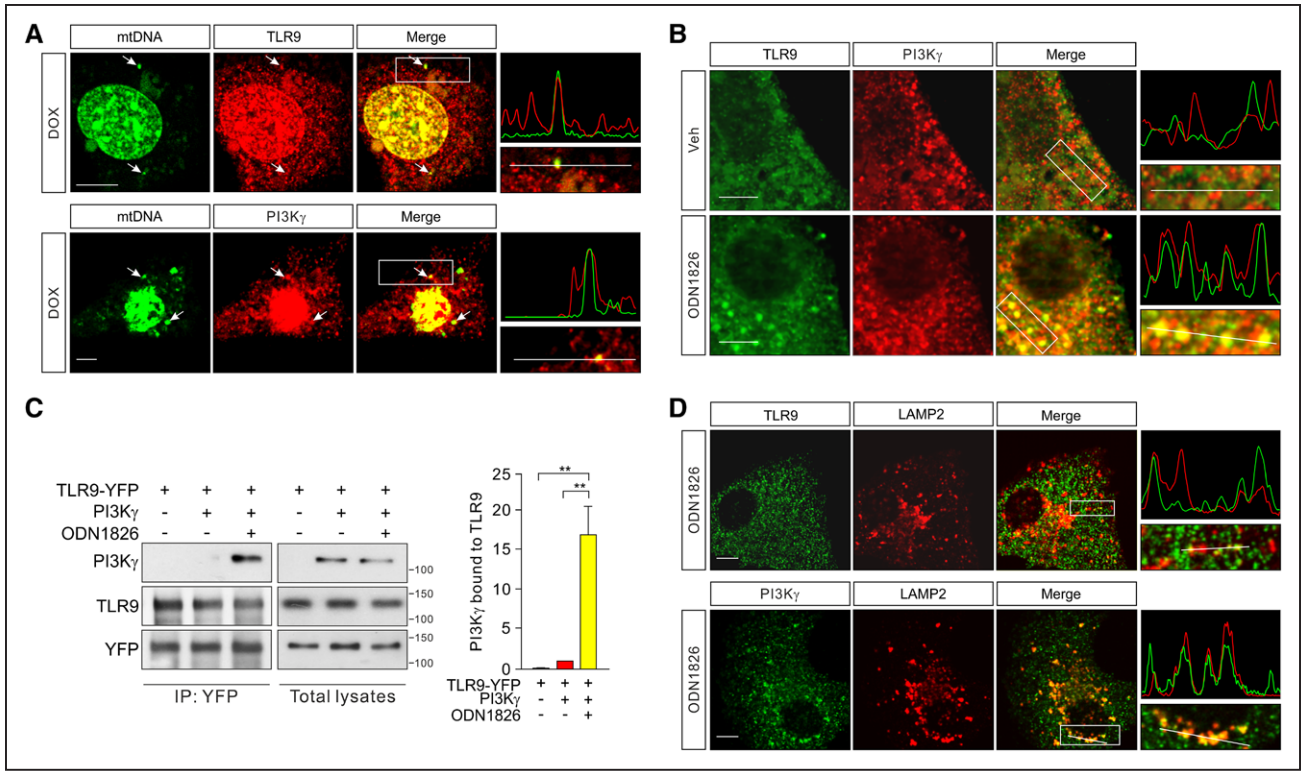

Figure 4. mtDNA, PI3Kγ, and TLR-9 colocalize in autolysosomes.
A, Double staining of mitochondrial DNA (mtDNA) and either TLR9 (red, upper) or PI3Kγ (red, bottom) in neonatal mouse ventricular myocytes (NMVMs) treated with doxorubicin (DOX, 1 μM) for 1 hour. Arrows indicate colocalization of mtDNA with either TLR9 or PI3Kγ. DOX has an intrinsic red fluorescence on nuclei. **B,** Double staining of TLR9 (green) and PI3Kγ (red) in NMVMs treated with vehicle or a CpG-rich oligonucleotide similar to mtDNA, ODN1826 (0.2 μM, 1 hour). **C,** Representative immunoblot (left) and relative quantification (right) of PI3Kγ bound to TLR9 in HEK-293 cells transfected with TLR9-YFP and PI3Kγ and treated with the TLR9 agonist ODN1826. Values represent mean±SEM, n≥4 independent experiments, $^{**}P<0.01$ by 1-way analysis of variance with Bonferroni post hoc test. **D,** Double staining of either TRL9 (green) or PI3Kγ (green) with the autolysosomal marker LAMP2 (red) in NMVMs treated with ODN1826 (0.2 μM, 1 hour). **A, B,** and **D,** Enlargements of the outlined areas and fluorescence intensity profiles in the green and red channels of the regions underneath the white lines (right). Scale bar, 5 μm. Representative pictures from n=3 experiments are shown. DOX indicates doxorubicin; KD, kinase-dead; LAMP2, lysosome-associated membrane protein 2; mtDNA, mitochondrial DNA; NMVMs, neonatal mouse ventricular myocytes; ODN1826, CpG oligodeoxynucleotide 1826; PI3Kγ, phosphoinositide 3-kinase γ; TLR9, toll-like receptor 9; Veh, vehicle; WT, wild-type; and YFP, yellow fluorescence protein.

TLR9 agonist, ODN1826, significantly elevated Akt phosphorylation in NMVMs (Figure 5A) and H9c2 cells (Figure VIB in the online-only Data Supplement). This effect was completely abolished by PI3Kγ inactivation in KD NMVMs (Figure 5A) and in AS605240-treated H9c2 cells (Figure VIB in the online-only Data Supplement).

Under stress conditions, engagement of the PI3K/Akt pathway may result in mTOR-mediated suppression of autophagy.[33] Therefore, activation of the autolysosomal TLR9/PI3Kγ/Akt signaling may provide a negative feedback regulation of autophagy. In H9c2 cells, DOX-mediated activation of Akt correlated with increased phosphorylation of mTOR targets, including S6 kinase, but also the autophagy inducer Ulk1 that is inactive when phosphorylated on Ser-757 (Figure VIA and VIC in the online-only Data Supplement).[34] In agreement, blockade of either TLR9 or PI3Kγ abrogated the inhibitory phosphorylation of Ulk1 (Figure VIA in the online-only Data Supplement). Conversely, direct activation of TRL9 with ODN1826 resulted in a PI3Kγ-dependent increase of Ulk1 phosphorylation (Figure VIB in the online-only Data Supplement). To confirm these observations in the heart of DOX-treated mice, activation of the PI3Kγ/mTOR pathway was studied by immunohistochemistry 3 days after treatment. Whereas WT hearts stained positive for phospho-Akt, phospho-mTOR, and phospho-Ulk1, no staining was detected in KD tissues (Figure 5B). This response was accompanied by the canonical TLR9-dependent transcriptional upregulation of inflammatory cytokines in WT but not KD hearts (Figure VID in the online-only Data Supplement), thus indicating a TLR9 involvement in vivo. In further agreement, inhibi-

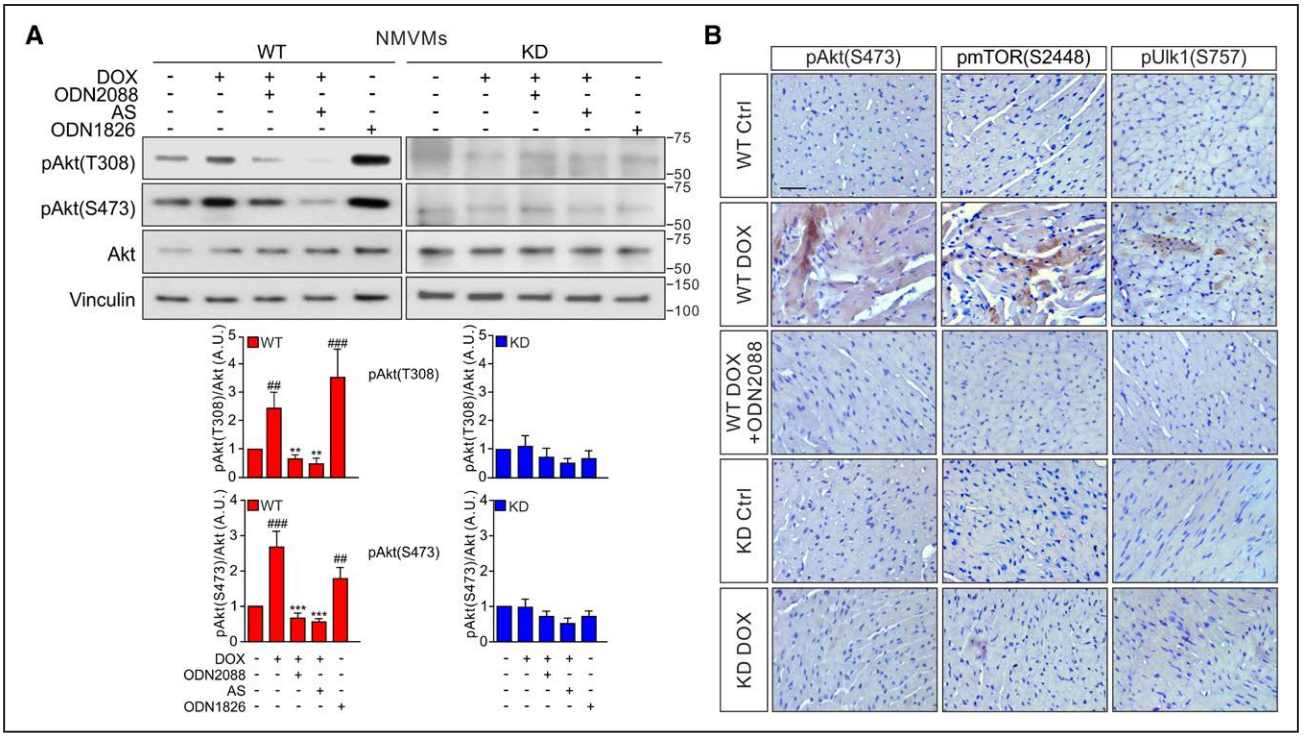

Figure 5. DOX activates a TLR9/PI3Kγ/Akt/Ulk1 pathway promoting feedback inhibition of autophagy.
A, WT and KD neonatal mouse ventricular myocytes (NMVMs) were treated with DOX (1 μmol/L, 1 hour) alone or in combination with the PI3Kγ inhibitor AS605240 (AS, 0.5 μmol/L, 1-hour pretreatment) or with the TLR9 antagonist ODN2088 (0.2 μmol/L, 5-hour pretreatment). Alternatively, NMVMs were stimulated with TLR9 agonist ODN1826 (0.2 μmol/L, 1 hour). Representative immunoblot (upper) and relative quantification (lower) of Akt phosphorylation on Thr308 (T308) and Ser473 (S473) residues are shown. DOX/ODN1826 versus vehicle: ##*P*<0.01 and ###*P*<0.001 and DOX+ODN2088/AS versus DOX: ***P*<0.01 and ****P*<0.001 by 1-way analysis of variance with Bonferroni post hoc test. n≥4 independent experiments. Values represent mean±SEM. **B,** Immunohistochemical analysis of the phosphorylation status of Akt (S473), mTOR (S2448), and Ulk1 (S757) in WT and KD hearts 3 days after a single injection of saline or doxorubicin (DOX, 4 mg/kg) alone or in combination with the TLR9 antagonist ODN2088 (100 μg/mouse). Scale bar, 100 μm. Representative pictures from n=3 experiments are shown. Akt indicates protein kinase B; AS, PI3Kγ inhibitor AS605240; ctrl, control; DOX, doxorubicin; KD, kinase-dead; mTOR, mechanistic target of rapamycin; NMVMs, neonatal mouse ventricular myocytes; ODN2088/1826, CpG oligodeoxynucleotide 2088/1826; PI3Kγ, phosphoinositide 3-kinase γ; TLR9, toll-like receptor 9; Ulk1, Unc-51 like autophagy activating kinase 1; and WT, wild-type.

tion of TLR9-mediated sensing of mtDNA by intravenous administration of the TLR9 antagonist ODN2088 blocked DOX-induced Akt/mTOR/Ulk1 signaling in WT hearts (Figure 5B).

Altogether these data indicate that DOX triggers an autolysosomal TLR9/PI3Kγ signaling converging on Ulk1 inactivation and, in turn, feedback inhibition of autophagy.

Inhibition of Autophagy in KD Mice Abrogates the Protection From DOX Cardiotoxicity

Resistance of KD mice to DOX-induced cardiotoxicity appeared linked to the loss of a negative feedback inhibiting autophagy. To test this hypothesis, autophagy was blocked genetically by an adeno-associated viral vector (AAV9) encoding a small hairpin RNA targeting the key autophagy initiating gene *Atg7* as well as a GFP probe labeling infected cells (AAV9-ATG7sh). Six weeks after infection, AAV9-ATG7sh led to a 45% reduction of cardiac *Atg7* mRNA levels (Figure VIIA in the online-only Data Supplement), and, as expected, KD animals either transduced with a control vector (AAV9-CTRLsh) or infected with AAV9-ATG7sh showed normal cardiac contractility (Figure 6A). Conversely, infection with the AAV9-ATG7sh significantly blunted the protection of KD mice against DOX-induced deterioration of fractional shortening (Figure 6A). In these hearts, the area of infected green cardiomyocytes was significantly lower than in noninfected controls (Figure 6B and 6C). Thus, genetic inhibition of cardiac autophagy abrogated the protection of PI3Kγ KD mice against DOX cardiotoxicity. Similar results were observed when autophagy was inhibited pharmacologically, with either BafA1, or compounds in clinical use, such as hydroxychloroquine. Similar to AAV9-ATG7sh, BafA1 and hydroxychloroquine im-

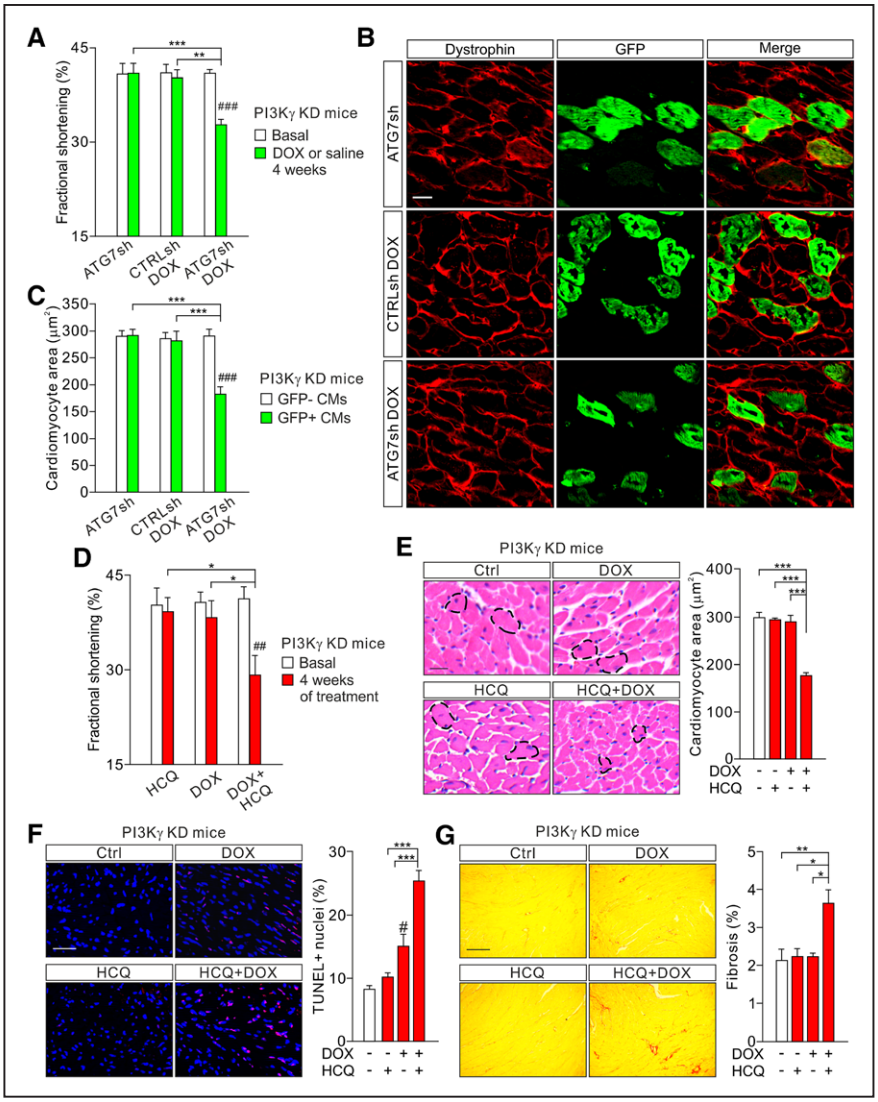

Figure 6. Genetic and pharmacological inhibition of autophagy abolishes cardioprotection in PI3Kγ KD mice. **A** through **C,** PI3Kγ KD mice were transduced with an adeno-associated viral vector (AAV9)-encoding GFP and either a small hairpin (sh) RNA against the *Atg7* gene (ATG7sh) or a control sh (CTRLsh) and treated with vehicle or doxorubicin (DOX, 4 mg/kg on days 0, 7, and 14). **A,** Fractional shortening before and 4 weeks after the first DOX injection is shown. 0 versus 4 weeks: ###*P*<0.001; ATG7sh DOX versus either CTRLsh DOX or ATG7sh saline: ***P*<0.01 and ****P*<0.001 by 2-way repeated-measures analysis of variance with Bonferroni post hoc test. ATG7sh, n=9; CTRLsh DOX, n=9; and ATG7sh DOX, n=9. **B,** Representative images of dystrophin and GFP staining in heart sections from KD mice treated as described in (**A**). Scale bar, 10 μm. **C,** Quantification of the area of GFP-positive cardiomyocytes (GFP+ CMs) and GFP-negative cardiomyocytes (GFP− CMs) in sections as shown in (**B**). GFP+ CMs versus GFP− CMs: ###*P*<0.001; ATG7sh DOX versus either ATG7sh or CTRLsh DOX: ****P*<0.001 by 2-way analysis of variance with Bonferroni post hoc test. **D** through **G,** KD mice were treated with doxorubicin (DOX, 4 mg/kg on days 0, 7, and 14; n=7), hydroxychloroquine (HCQ, 60 mg/kg daily from days 0–28; n=7), or a combination of DOX and HCQ (n=9). **D,** Fractional shortening before and 4 weeks after the first DOX injection is shown. Before versus after the treatment: ##*P*<0.01 and DOX+HCQ versus single treatments (DOX or HCQ): **P*<0.05 by 2-way repeated-measures analysis of variance with Bonferroni post hoc test. **E,** Representative images of H&E staining (left) and quantification of cardiomyocyte area (right) in KD hearts 4 weeks after the first dose of DOX or saline. Scale bar, 20 μm. **F,** Representative images of TUNEL staining (left) and quantification of TUNEL-positive nuclei per field (right) in KD whole hearts treated as in (**D**). Scale bar, 30 μm. **G,** Representative images of PicroSirius Red staining (left) and relative quantification of collagen deposition (right) in heart sections from KD animals treated as in (**D**). Scale bar, 50 μm. **E** through **G**, DOX+HCQ versus single treatments (DOX or HCQ): **P*<0.05, ***P*<0.01, and ****P*<0.001; and DOX versus saline: #*P*<0.05 by 2-way analysis of variance with Bonferroni post hoc test. Values represent mean±SEM. AAV9 indicates adeno-associated viral vector; ATG7sh, AAV9-encoding GFP and small hairpin (sh) RNA against the Atg7 gene; CMs, cardiomyocytes; Ctrl, control; CTRLsh, AAV9-encoding GFP and small hairpin (sh) RNA against control gene; DOX, doxorubicin; GFP, green fluorescence protein; HCQ, hydroxychloroquine; KD, kinase-dead; PI3Kγ, phosphoinositide 3-kinase γ; TUNEL, terminal deoxynucleotidyl transferase dUTP nick end labeling; and WT, wild-type.

paired cardiac contractility in DOX-treated KD mice (Figure 6D and Figure VIIB in the online-only Data Supplement) and restored their susceptibility to DOX-induced cardiomyocyte atrophy, apoptosis, and myocardial fibrosis (Figure 6E through 6G).

To test whether enhanced autophagy triggered by PI3Kγ inhibition protects against other known DOX-induced toxic effects,[35] disruption of mitochondrial membrane potential, Ca^{2+} mishandling, reactive oxygen species (ROS) production and DNA damage were studied. In DOX-treated WT cardiomyocytes, the PI3Kγ inhibitor AS605240 but not the combination of this drug with the autophagy blocker BafA1 prevented both the impairment of mitochondrial membrane potential and the induction of spontaneous Ca^{2+} waves (Figure VIIIA and VIIIB in the online-only Data Supplement). Furthermore, KD hearts and AS605240-treated NMVMs showed significant protection against DOX-induced ROS production and DNA damage, which was abrogated by blocking autophagy with either BafA1 or an adenovirus harboring an ATG7 small hairpin RNA (Figure VIIIC through VIIIE in the online-only Data Supplement).

Altogether these results corroborate the view that PI3Kγ inhibition protects against DOX cardiotoxicity by unleashing autophagy.

PI3Kγ Inhibition Potentiates the Anticancer Activity of Anthracyclines by Restoring Antitumor Immune Responses

To evaluate the potential use of PI3Kγ inhibitors as cardioprotectants in the context of anthracycline therapy, the combined effect of DOX and PI3Kγ inhibition on tumor growth was explored. DOX-sensitive 4T1 breast cancer cells, which do not express PI3Kγ,[36] were initially studied. Accordingly, in vitro administration to 4T1 cells of the PI3Kγ inhibitor AS605240 did not affect growth (Figure IXA in the online-only Data Supplement), but treatment of the same cells with DOX resulted in a concentration-dependent lethality (Figure IXB in the online-only Data

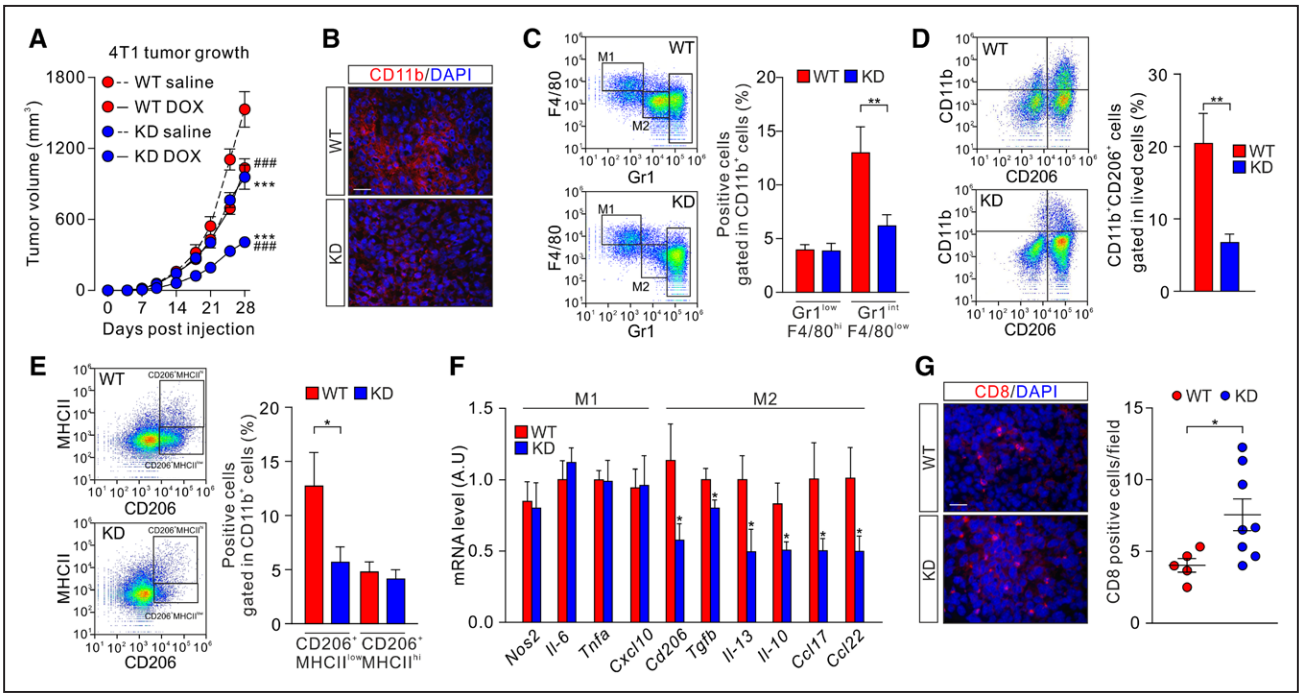

Figure 7. PI3Kγ inhibition potentiates the anticancer activity of DOX by restoring antitumor immune responses. **A,** Tumor growth in WT and KD mice injected with 1x10^5 4T1 breast cancer cells and treated with a cumulative dose of doxorubicin (DOX, 12 mg/kg) or saline via 3 weekly injections (4 mg/kg on days 0, 7, and 14). n=12 to 20 animals/group. Saline versus DOX: ###*P*<0.001; and WT versus KD: ****P*<0.001 by 2-way repeated-measures analysis of variance with Bonferroni post hoc test. **B,** Representative immunofluorescence staining from n=3 experiments of the myeloid marker CD11b in 4T1 tumors from WT and KD mice treated as in (**A**). Scale bar, 30 μm. **C,** Representative FACS plots (left) and relative quantification (right) of Gr1^{low}F4/80^{hi} (antitumor) and Gr1^{int}F4/80^{low} (protumor) macrophages in 4T1 tumors from mice treated as in (**A**). **D** and **E,** Representative FACS plots (left) and relative quantification (right) of CD206$^+$ protumor macrophages (**D**), characterized by low MHC-II expression (CD206$^+$MHC^{low}) (**E**) in 4T1 tumors from mice treated as in (**A**). **F,** Relative mRNA expression of antitumor and protumor cytokines in 4T1 tumors from mice treated as in (**A**). **G,** Representative immunofluorescence images (left) and relative quantification (right) of CD8$^+$ T cells in 4T1 tumors from mice treated as in (**A**). Scale bar, 30 μm. **C**–**G**, n=5 to 8 animals/group. **C** and **E**, **P*<0.05 by 2-way analysis of variance with Bonferroni post hoc test. **D, F,** and **G,** **P*<0.05 and ***P*<0.01 by Student's *t* test. Values represent mean±SEM. DOX indicates doxorubicin; KD, kinase-dead; M1, classically activated antitumoral macrophages; M2, alternatively activated protumoral macrophages; PI3Kγ, phosphoinositide 3-kinase γ; and WT, wild-type.

Supplement). Nonetheless, 4T1 cells grew in vivo significantly less in KD than in WT mice (Figure 7A), and DOX further delayed tumor growth, leading to significantly smaller tumors in KD than in WT mice (Figure 7A).

Because PI3Kγ regulates cancer immune suppression,[8,9] to understand how PI3Kγ inhibition synergizes with DOX, tumor-associated leukocytes were analyzed. CD11b immunostaining revealed reduced myeloid infiltration in 4T1 tumors implanted in KD recipients (Figure 7B). Fluorescence-activated cell sorting analysis on CD11b$^+$ cells from the same tumors confirmed a lower number of Gr1^{int}F4/80^{low} protumor macrophages in KD than in WT, whereas Gr1^{low}F4/80^{hi} antitumor macrophages were unchanged (Figure 7C). To better characterize this population, the expression of CD206, in combination with that of MHC class II molecule, was analyzed.[37] The percentage of CD206$^+$ cells (Figure 7D) characterized by low MHC-II expression (Figure 7E), showing a phenotype typically associated to protumor macrophages, was significantly lower in tumors grown in KD than in WT recipients. In line with reduced recruitment of protumor macrophages, KD tumors expressed significantly smaller

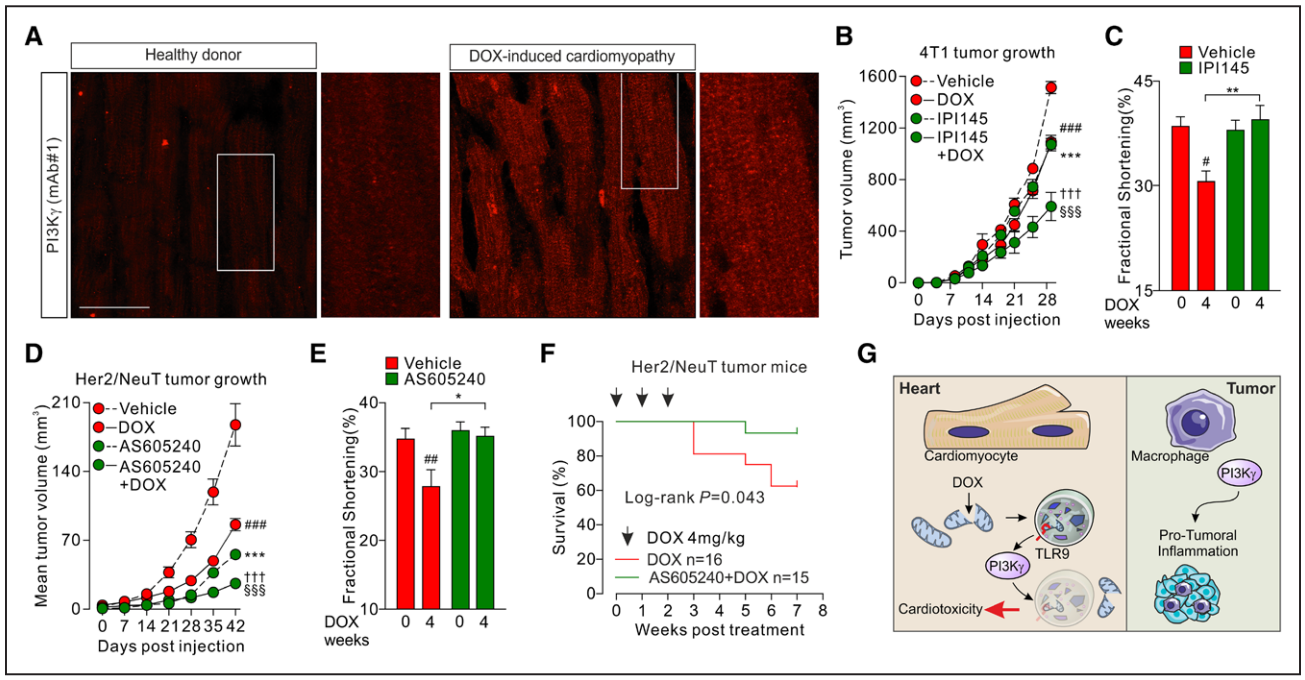

Figure 8. Pharmacological inhibition of PI3Kγ simultaneously prevents cardiomyopathy and tumor growth under DOX treatment.

A, PI3Kγ staining in human heart sections from a healthy donor (left) and a patient who developed cardiomyopathy after doxorubicin (DOX) treatment (right) (details in online-only Data Supplement). Enlargements of the outlined areas (right). Scale bar, 50 μm. **B** and **C,** WT and KD mice were injected with 1×10^5 4T1 breast cancer cells and treated with doxorubicin (DOX) or saline via 3 weekly injections (4 mg/kg on days 0, 7, and 14). The PI3Kγ inhibitor IPI145 or vehicle was administered daily for 3 weeks since the first DOX injection. **B,** Tumor growth is shown. Animals/group: vehicle, n=6; IPI145, n=6; DOX, n=12; IPI145+DOX, n=12. DOX versus vehicle: ###P<0.001; IPI145 versus vehicle: ***P<0.001; DOX+IPI145 versus DOX: †††P<0.001; DOX+IPI145 versus IPI145: §§§P<0.001 by 2-way repeated-measures analysis of variance with Bonferroni post hoc test. **C,** Fractional shortening of animals treated with vehicle+DOX (n=12) and IPI145+DOX (n=12). 0 versus 4 weeks after DOX: #P<0.05 and vehicle versus IPI145: **P<0.01 by 2-way repeated-measures analysis of variance with Bonferroni post hoc test. Values represent mean±SEM. **D** through **F,** Her2/NeuT transgenic mice bearing spontaneous tumors (2 mm in mean diameter) were administered with saline or DOX as above, together with daily treatment with vehicle or the PI3Kγ inhibitor AS605240 (AS) for 3 weeks since the first DOX injection. **D,** Growth curve of Her2/NeuT tumors in all mammary glands. Mean tumor volume per mammary gland is shown. Animals/group: vehicle, n=6; AS605240, n=6; DOX, n=16; AS605240+DOX, n=15. DOX versus vehicle: ###P<0.001; AS605240 versus vehicle: ***P<0.001; DOX+AS605240 versus DOX: †††P<0.001; DOX+ AS605240 versus AS605240: §§§P<0.001 by 2-way repeated-measures analysis of variance with Bonferroni post hoc test. **E,** Fractional shortening of Her2/NeuT mice treated with vehicle+DOX (n=8) or AS605240+DOX (n=8). 0 versus 4 weeks after DOX: ##P<0.01 and vehicle versus AS605240: *P<0.01 by 2-way repeated-measures analysis of variance with Bonferroni post hoc test. Values represent mean±SEM. **F,** Kaplan–Meier survival curves of Her2/NeuT mice treated with vehicle+DOX (n=16) and AS605240+DOX (n=15). Arrows indicate DOX injections. Log-rank test was used for statistical analysis. **G,** Schematic representation of the diverse function of PI3Kγ in cardiomyocytes and tumor-associated macrophages during anthracycline therapy. (Left) In the heart, DOX-damaged mitochondrial DNA activates autolysosomal TLR9/PI3Kγ pathway and engages feedback inhibition of autophagy, resulting in the accumulation of damaged mitochondria and cardiotoxicity. (Right) In the tumor microenvironment, macrophage PI3Kγ mediates protumoral inflammation and promotes tumor growth. DOX indicates doxorubicin; PI3Kγ, phosphoinositide 3-kinase γ; and TLR9, toll-like receptor 9.

amounts of protumor cytokines (*Tgfb*, *Il-13*, *Il-10*, *Ccl17*, and *Ccl22*) than WT, whereas antitumor signals were not different between the 2 groups (Figure 7F). In accordance with the immune-suppressive action of protumor macrophages,[38] tumor-killing CD8+ T cells were more abundant in tumors from KD than from WT mice (Figure 7G).

Overall, these data indicate that inhibition of PI3Kγ synergizes with the antitumor action of DOX by interfering with the recruitment of protumor macrophages and eventually unleashing antitumor T-cell responses.

PI3Kγ Inhibition Simultaneously Prevents Cardiotoxicity and Tumor Growth Under Anthracycline Treatment

The clinical translatability of PI3Kγ inhibition was evaluated next. PI3Kγ protein expression was analyzed in human heart sections from a patient who developed severe DOX-induced cardiomyopathy requiring heart transplantation. Immunofluorescence assays revealed higher and more punctate expression of the catalytic p110γ subunit in DOX-damaged hearts than in healthy controls (Figure 8A and Figure XA and XB in the online-only Data Supplement), highlighting a correlation between PI3Kγ upregulation and DOX-induced cardiotoxicity. PI3Kγ upregulation might also occur in other more easily accessible tissues and potentially represent a biomarker of DOX-induced cardiotoxicity. In silico analysis of *PIK3CG* (encoding p110γ) mRNA levels in blood samples from patients subjected to anthracycline chemotherapy showed that *PIK3CG* mRNA was 50% more abundant in patients who developed heart disease after anthracycline treatment (group 3) than in healthy controls (group 1). No *PIK3CG* upregulation was detected in subjects showing normal heart function after chemotherapy (group 2) (relative *PIK3CG* mRNA level: group 1=1.00±0.02, group 2=1.09±0.09, group 3=1.52±0.16; group 3 versus group 2: $P<0.05$ by 1-way ANOVA with Bonferroni post hoc test). This modulation appeared isoform-specific because the mRNA levels of *PIK3CA* (the gene encoding the p110α catalytic subunit of PI3Kα, the most abundant cardiac PI3K isoform) were not affected by DOX (relative *PIK3CA* mRNA level: group 1=1.00±0.06, group 2=1.12±0.07, group 3=1.02±0.05; no significance among groups by 1-way ANOVA with Bonferroni post hoc test). Overall, these data provide preliminary evidence that aberrant expression and activation of PI3Kγ may correlate with DOX cardiotoxicity in human patients.

The ability of PI3Kγ inhibition to delay tumor growth and, at the same time, protect the heart during DOX treatment was assessed in preclinical models of breast cancers. Consistent with the findings in tumor-free animals, KD mice bearing a tumor derived by the injection of either 4T1 or TUBO mammary gland cancer cells were protected against DOX-induced remodeling and contractile dysfunction (Figures XIA and XIB and XIIA through XIIC and Table V in the online-only Data Supplement). With both cell lines, the tumor led to 50% of mortality in WT mice, but significantly higher survival was observed in KD mice (Figure XIC and XID in the online-only Data Supplement). Thus, PI3Kγ inactivation improves survival by limiting tumor growth and concomitantly prevents DOX cardiotoxicity.

Next, the ability of pharmacological inhibition of PI3Kγ to recapitulate the protection observed in the genetic model was explored. AS605240 significantly prevented DOX-induced contractile dysfunction, cardiomyocyte atrophy, and apoptosis as well as myocardial fibrosis in tumor-free mice (Figure XIIIA through XIIIC and Table VI in the online-only Data Supplement). Similarly, the more clinically advanced PI3Kγ (and PI3Kδ) inhibitor IPI-145[14] delayed tumor growth per se and potentiated the antitumor effect of DOX (Figure 8B) while preventing DOX-induced contractile dysfunction (Figure 8C) in 4T1 tumor-bearing animals. The dual therapeutic potential of PI3Kγ inhibitors was validated in a model of spontaneous mammary tumor growth. Her2/NeuT tumors grew significantly less in mice treated with AS605240 compared with vehicle, and the PI3Kγ inhibitor synergized with DOX when administered in combination (Figure 8D). The antitumor effects of AS605240 were accompanied by cardioprotection of DOX-treated mice (Figure 8E and Figure XIID through XIIF in the online-only Data Supplement) and ultimately resulted in significantly lower mortality than in vehicle-treated animals (Figure 8F).

Altogether these data uncover PI3Kγ inhibition as a unique means of synergizing with the antitumor activity of standard chemotherapy while defending the heart from the iatrogenic cardiotoxicity.

DISCUSSION

The present study uncovers PI3Kγ as a major player of anthracyclines cardiotoxicity and proposes PI3Kγ inhibition as an effective means of preventing the cardiac side effects of DOX while boosting its anticancer action.

Despite major efforts in understanding the mechanism of anthracyclines-induced cardiotoxicity, molecular and cellular details are not yet fully understood. Potential mechanisms include generation of ROS and targeting of topoisomerase II-β, together leading to DNA damage, mitochondrial dysfunction, and Ca^{2+} mishandling.[13,39,40] Yet the ROS-scavenging iron chelator and topoisomerase II-β modulator dexrazoxane failed to provide significant benefit, suggesting the existence of additional factors. Whether PI3Kγ, a well-known inducer of maladaptive responses in various cardiac conditions,[11,41,42] was involved in DOX-elicited cardiotoxicity has remained unknown so far. Our findings now fill this

gap and support PI3Kγ-mediated block of autophagy as a major driver of DOX-evoked cardiotoxicity.

Although the role of cardiac autophagy in anthracyclines cardiotoxicity has been the subject of debate,[43,44] our results support the notion that DOX impairs but does not abolish the autophagic flux in cardiomyocytes[26] and that this reduction is detrimental to the heart.[42,45] Our study also indicates that DOX-related cardiomyopathy can be prevented by the stimulation of autophagy, likely driving efficient disposal of damaged mitochondria, the major sites of DOX-induced ROS production.[26,29,46] Consistent with this view, our findings showed that the prompt clearance of injured and potentially harmful organelles ensured a general protection against ROS-related toxic effects, including DNA damage, Ca^{2+} mishandling, and disruption of mitochondrial metabolism.

Nonetheless, activation of PI3Kγ was found to trigger a negative feedback loop eventually inhibiting autophagy. Mitochondrial damage elicited by DOX led to an initial mitochondrial autophagy, which stimulated PI3Kγ through the activation of endosomal TLR9, a receptor sensing CpG-rich mtDNA released in autolysosomes.[17] This finding was unexpected, especially in view of the classic role played by PI3Kγ signaling downstream of G protein-coupled receptors.[47] Conversely, this result appeared in agreement with studies showing PI3Kγ being noncanonically activated downstream of TLRs[30] and being localized in endosomes.[31] Our findings showed that in the absence of PI3Kγ, TLR9 signaling is severely impaired and the TLR9-dependent cytokine production is decreased. However, whereas in pressure-overloaded hearts TLR9 engagement by mitochondrial damage initiates inflammation, leukocyte infiltration, and, ultimately, maladaptive cardiac remodeling,[17] leukocyte recruitment to the myocardium is almost negligible in DOX-induced cardiomyopathy.[48] Instead, TLR9-mediated activation of PI3Kγ converged on the feedback inhibition of autophagy (Figure 8G) and the concomitant metabolic reprogramming of cardiomyocytes. This likely represents an attempt of PI3Kγ to cope with the cardiac damage elicited by chemotherapy through a 2-pronged action. On the one hand, the block of autophagy may avoid the accumulation of potentially harmful undegraded autolysosomes.[26,45] This situation is likely to occur in DOX-treated hearts, where lysosomes are dysfunctional and cannot properly deal with an exaggerated autophagosome formation.[26,45] On the other hand, PI3Kγ activation may be poised to interrupt the vicious cycle of ROS formation by injured organelles by promoting a switch toward a more ROS-sparing, nonmitochondrial metabolism. Although these PI3Kγ-directed events may be initially compensatory, anaerobic glycolysis may eventually fail to sustain cardiac energy demand and, together with impaired autophagic disposal of injured mitochondria, may lead to metabolic derangement and cardiotoxicity. This metabolic switch and its long-term consequences can account for the emergence of cardiac damage long after completion of anthracyclines treatment.

Pharmacological interference with PI3Kγ-dependent signaling in cardiomyocytes may indirectly improve cancer prognosis by increasing tolerability of cardiotoxic anticancer treatments. PI3Kγ inhibitors also display major antineoplastic properties and are thus particularly attractive dual-action therapeutic agents for cancer patients. PI3Kγ does not impact tumor growth directly but promotes both the trafficking and differentiation of a subset of immunosuppressive protumor macrophages, which ultimately block T-cell–mediated tumor killing.[8,10] Accordingly, PI3Kγ inactivation unleashes adaptive immunity and delays tumor growth per se but also allows overcoming resistance to immune checkpoint-blocking antibodies.[8,10] How PI3Kγ-directed immunity interacts with anthracyclines is unknown. The present study demonstrates that PI3Kγ inhibitors not only synergize with antitumor effects of DOX but also concomitantly defend the heart from iatrogenic cardiotoxicity.

This cardioprotective approach is potentially applicable to most patients undergoing anthracyclines-based regimens, including pediatric leukemia patients, for whom long-term cardiotoxicity is a devastating complication during adulthood.[49] Similarly, this applies to breast cancer patients exposed to the highly effective but extremely cardiotoxic combination of anthracyclines and anti-ErbB2 monoclonal antibodies.[50] Cardioprotective strategies may potentially allow cancer chemotherapies in frail, elderly individuals, even in the presence of preexisting cardiac diseases. Our finding that patients with DOX-induced cardiac toxicity showed overexpression of PI3Kγ further indicates that targeting this kinase might be effective in mouse models as well as patients. Inhibition of PI3Kγ may represent an attractive approach, especially because IPI-145, the oral PI3Kγ/δ dual inhibitor used in this study,[14] is currently undergoing a phase III clinical trial for hematologic malignancies, and another more selective PI3Kγ inhibitor, IPI-549,[51] is now approaching phase I clinical evaluation.

Overall, PI3Kγ inhibition may improve the prognosis of patients with cancer treated with DOX by concomitantly unleashing antitumor immunity as well as preventing cardiotoxicity. Therefore, PI3Kγ inhibitors might eventually help to "kill two birds with one stone" in patients with cancer requiring anthracycline chemotherapy.

ARTICLE INFORMATION

Received July 4, 2017; accepted December 20, 2017.

The online-only Data Supplement is available with this article at https://www.ahajournals.org/doi/suppl/10.1161/CIRCULATIONAHA.117.030352.

Authors

Mingchuan Li, PhD; Valentina Sala, PhD; Maria Chiara De Santis, MS; James Cimino, BS; Paola Cappello, PhD; Nicola Pianca, PhD; Anna Di Bona, MS; Jean Piero Margaria, MS; Miriam Martini, PhD; Edoardo Lazzarini, PhD; Flora Pirozzi,

MD, PhD; Luca Rossi, BS; Irene Franco, PhD; Julia Bornbaum, PhD; Jacqueline Heger, PhD; Susanne Rohrbach, PhD; Alessia Perino, PhD; Carlo G. Tocchetti, MD, PhD; Braulio H.F. Lima, PhD; Mauro M. Teixeira, MD, PhD; Paolo E. Porporato, PhD; Rainer Schulz, MD, PhD; Annalisa Angelini, MD, PhD; Marco Sandri, PhD; Pietro Ameri, MD, PhD; Sebastiano Sciarretta, MD, PhD; Roberto César P. Lima-Júnior, PhD; Marco Mongillo, MD, PhD; Tania Zaglia, PhD; Fulvio Morello, MD, PhD; Francesco Novelli, PhD; Emilio Hirsch, PhD*; Alessandra Ghigo, PhD*

Correspondence

Emilio Hirsch, PhD, Department of Molecular Biotechnology and Health Sciences, Molecular Biotechnology Center, University of Torino, Via Nizza 52, 10126, Torino, Italy; or Alessandra Ghigo, PhD, Department of Molecular Biotechnology and Health Sciences, Molecular Biotechnology Center, University of Torino, Via Nizza 52, 10126, Torino, Italy. E-mail emilio.hirsch@unito.it or alessandra.ghigo@unito.it

Affiliations

Department of Molecular Biotechnology and Health Sciences, Molecular Biotechnology Center, University of Torino, Italy (M.L., V.S., M.C.D.S., J.C., J.P.M., M.M., F.P., L.R., I.F., A.P., P.E.P., R.C.P.L.-J., E.H., A.G.). Center for Experimental Research and Medical Studies, Azienda Ospedaliera Universitaria Città della Salute e della Scienza di Torino, Italy (P.C., F.N.). Department of Biomedical Sciences, University of Padova, Italy (N.P., A.D.B., M.S., M.M., T.Z.). Venetian Institute of Molecular Medicine, Padova, Italy (N.P., A.D.B., M.S., M.M., T.Z.). Department of Cardiac, Thoracic, and Vascular Sciences, University of Padova, Italy (A.D.B., A.A., T.Z.). Department of Internal Medicine, Cardiovascular Biology Laboratory, University of Genova and IRCCS Policlinic Hospital San Martino, Italy (E.L., P.A.). Department of Translational Medical Sciences, Division of Internal Medicine, Federico II University, Napoli, Italy (F.P., C.G.T.). Institut für Physiologie, Justus Liebig University Giessen, Germany (J.B., J.H., S.R., R.S.). Departamento de Bioquímica e Imunologia, Instituto de Ciências Biológicas, Universidade Federal de Minas Gerais, Belo Horizonte, Minas Gerais, Brazil (B.H.F.L., M.M.T.). Department of Medical and Surgical Sciences and Biotechnologies, University of Rome Sapienza, Latina, Italy (S.S.). Department of Physiology and Pharmacology, Laboratory of Pharmacology of Inflammation and Cancer, Universidade Federal do Ceará/UFC, Fortaleza, Brazil (R.C.P.L.-J.). A.O.U. Città della Salute e della Scienza di Torino, S.C. Emergency Medicine, Torino, Italy (V.S., F.M.).

Sources of Funding

This work was supported by grants from Progetto d'Ateneo-Compagnia di San Paolo (PICANCAR to A.G., PANTHER to P.C., and PC-METAIMMUNOTHER to F.N.), 2013 International Society for Heart Research/Servier Research Fellowship (to A.G.), Italian Ministry of Health (no. GR-2013-02355449 to F.M. and RF-2013-02354892 to F.N.), Associazione Italiana Ricerca sul Cancro (5 x mille no. 12182 and IG no. 15257 to F.N.), and Leducq Foundation (no. 09CVD01 to E.H.). M.L. received a PhD studentship award from the Chinese Scholarship Council. M.M. is supported by a Fondazione Umberto Veronesi fellowship. R.C.P.L.-J. is supported by a Capes Fellowship (Estágio Sênior no Exterior-Processo nº 88881.119732/2016-01) and by PRONEX/FUNCAP/CNPq (PR2-0101-00054.01.00/15).

Disclosures

Dr Hirsch is a cofounder of Kither Biotech S.r.l., an academic spinoff involved in the development of PI3K inhibitors. The other authors report no conflicts of interest.

REFERENCES

1. Zamorano JL, Lancellotti P, Rodriguez Muñoz D, Aboyans V, Asteggiano R, Galderisi M, Habib G, Lenihan DJ, Lip GY, Lyon AR, Lopez Fernandez T, Mohty D, Piepoli MF, Tamargo J, Torbicki A, Suter TM; Authors/Task Force Members; ESC Committee for Practice Guidelines (CPG). 2016 ESC position paper on cancer treatments and cardiovascular toxicity developed under the auspices of the ESC Committee for Practice Guidelines: the task force for cancer treatments and cardiovascular toxicity of the European Society of Cardiology (ESC). *Eur Heart J*. 2016;37:2768–2801. doi: 10.1093/eurheartj/ehw211.
2. Cardinale D, Colombo A, Bacchiani G, Tedeschi I, Meroni CA, Veglia F, Civelli M, Lamantia G, Colombo N, Curigliano G, Fiorentini C, Cipolla CM. Early detection of anthracycline cardiotoxicity and improvement with heart failure therapy. *Circulation*. 2015;131:1981–1988. doi: 10.1161/CIRCULATIONAHA.114.013777.
3. Lipshultz SE, Scully RE, Lipsitz SR, Sallan SE, Silverman LB, Miller TL, Barry EV, Asselin BL, Athale U, Clavell LA, Larsen E, Moghrabi A, Samson Y, Michon B, Schorin MA, Cohen HJ, Neuberg DS, Orav EJ, Colan SD. Assessment of dexrazoxane as a cardioprotectant in doxorubicin-treated children with high-risk acute lymphoblastic leukaemia: long-term follow-up of a prospective, randomised, multicentre trial. *Lancet Oncol*. 2010;11:950–961. doi: 10.1016/S1470-2045(10)70204-7.
4. Tebbi CK, London WB, Friedman D, Villaluna D, De Alarcon PA, Constine LS, Mendenhall NP, Sposto R, Chauvenet A, Schwartz CL. Dexrazoxane-associated risk for acute myeloid leukemia/myelodysplastic syndrome and other secondary malignancies in pediatric Hodgkin's disease. *J Clin Oncol*. 2007;25:493–500. doi: 10.1200/JCO.2005.02.3879.
5. Vanhaesebroeck B, Guillermet-Guibert J, Graupera M, Bilanges B. The emerging mechanisms of isoform-specific PI3K signalling. *Nat Rev Mol Cell Biol*. 2010;11:329–341. doi: 10.1038/nrm2882.
6. Perino A, Ghigo A, Ferrero E, Morello F, Santulli G, Baillie GS, Damilano F, Dunlop AJ, Pawson C, Walser R, Levi R, Altruda F, Silengo L, Langeberg LK, Neubauer G, Heymans S, Lembo G, Wymann MP, Wetzker R, Houslay MD, Iaccarino G, Scott JD, Hirsch E. Integrating cardiac PIP3 and cAMP signaling through a PKA anchoring function of p110γ. *Mol Cell*. 2011;42:84–95. doi: 10.1016/j.molcel.2011.01.030.
7. Damilano F, Franco I, Perrino C, Schaefer K, Azzolino O, Carnevale D, Cifelli G, Carullo P, Ragona R, Ghigo A, Perino A, Lembo G, Hirsch E. Distinct effects of leukocyte and cardiac phosphoinositide 3-kinase γ activity in pressure overload-induced cardiac failure. *Circulation*. 2011;123:391–399. doi: 10.1161/CIRCULATIONAHA.110.950543.
8. Kaneda MM, Messer KS, Ralainirina N, Li H, Leem CJ, Gorjestani S, Woo G, Nguyen AV, Figueiredo CC, Foubert P, Schmid MC, Pink M, Winkler DG, Rausch M, Palombella VJ, Kutok J, McGovern K, Frazer KA, Wu X, Karin M, Sasik R, Cohen EE, Varner JA. PI3Kγ is a molecular switch that controls immune suppression. *Nature*. 2016;539:437–442. doi: 10.1038/nature19834.
9. Kaneda MM, Cappello P, Nguyen AV, Ralainirina N, Hardamon CR, Foubert P, Schmid MC, Sun P, Mose E, Bouvet M, Lowy AM, Valasek MA, Sasik R, Novelli F, Hirsch E, Varner JA. Macrophage PI3Kγ drives pancreatic ductal adenocarcinoma progression. *Cancer Discov*. 2016;6:870–885. doi: 10.1158/2159-8290.CD-15-1346.
10. De Henau O, Rausch M, Winkler D, Campesato LF, Liu C, Cymerman DH, Budhu S, Ghosh A, Pink M, Tchaicha J, Douglas M, Tibbitts T, Sharma S, Proctor J, Kosmider N, White K, Stern H, Soglia J, Adams J, Palombella VJ, McGovern K, Kutok JL, Wolchok JD, Merghoub T. Overcoming resistance to checkpoint blockade therapy by targeting PI3Kγ in myeloid cells. *Nature*. 2016;539:443–447. doi: 10.1038/nature20554.
11. Patrucco E, Notte A, Barberis L, Selvetella G, Maffei A, Brancaccio M, Marengo S, Russo G, Azzolino O, Rybalkin SD, Silengo L, Altruda F, Wetzker R, Wymann MP, Lembo G, Hirsch E. PI3Kγ modulates the cardiac response to chronic pressure overload by distinct kinase-dependent and -independent effects. *Cell*. 2004;118:375–387. doi: 10.1016/j.cell.2004.07.017.
12. Quaglino E, Iezzi M, Mastini C, Amici A, Pericle F, Carlo ED, Pupa SM, Giovanni CD, Spadaro M, Curcio C, Lollini PL, Musiani P, Forni G, Cavallo F. Electroporated DNA vaccine clears away multifocal mammary carcinomas in Her-2/neu transgenic mice. *Cancer Res*. 2004;64:2858–2864.
13. Zhao Y, McLaughlin D, Robinson E, Harvey AP, Hookham MB, Shah AM, McDermott BJ, Grieve DJ. Nox2 NADPH oxidase promotes pathologic cardiac remodeling associated with Doxorubicin chemotherapy. *Cancer Res*. 2010;70:9287–9297. doi: 10.1158/0008-5472.CAN-10-2664.
14. Winkler DG, Faia KL, DiNitto JP, Ali JA, White KF, Brophy EE, Pink MM, Proctor JL, Lussier J, Martin CM, Hoyt JG, Tillotson B, Murphy EL, Lim AR, Thomas BD, Macdougall JR, Ren P, Liu Y, Li LS, Jessen KA, Fritz CC, Dunbar JL, Porter JR, Rommel C, Palombella VJ, Changelian PS, Kutok JL. PI3K-δ and PI3K-γ inhibition by IPI-145 abrogates immune responses and suppresses activity in autoimmune and inflammatory disease models. *Chem Biol*. 2013;20:1364–1374. doi: 10.1016/j.chembiol.2013.09.017.
15. Schmid MC, Avraamides CJ, Dippold HC, Franco I, Foubert P, Ellies LG, Acevedo LM, Manglicmot JR, Song X, Wrasidlo W, Blair SL, Ginsberg MH, Cheresh DA, Hirsch E, Field SJ, Varner JA. Receptor tyrosine kinases and TLR/IL1Rs unexpectedly activate myeloid cell PI3kγ, a single convergent point promoting tumor inflammation and progression. *Cancer Cell*. 2011;19:715–727. doi: 10.1016/j.ccr.2011.04.016.
16. Ghigo A, Perino A, Mehel H, Zahradníková A, Morello F, Leroy J, Nikolaev VO, Damilano F, Cimino J, Luca ED, Richter W, Westenbroek R, Catterall

WA, Zhang J, Yan C, Conti M, Gomez AM, Vandecasteele G, Hirsch E, Fischmeister R. Phosphoinositide 3-kinase γ protects against catecholamine-induced ventricular arrhythmia through protein kinase A: mediated regulation of distinct phosphodiesterases. *Circulation*. 2012;126:2073–2083. doi: 10.1161/CIRCULATIONAHA.112.114074.
17. Oka T, Hikoso S, Yamaguchi O, Taneike M, Takeda T, Tamai T, Oyabu J, Murakawa T, Nakayama H, Nishida K, Akira S, Yamamoto A, Komuro I, Otsu K. Mitochondrial DNA that escapes from autophagy causes inflammation and heart failure. *Nature*. 2012;485:251–255. doi: 10.1038/nature10992.
18. Zaglia T, Milan G, Franzoso M, Bertaggia E, Pianca N, Piasentini E, Voltarelli VA, Chiavegato D, Brum PC, Glass DJ, Schiaffino S, Sandri M, Mongillo M. Cardiac sympathetic neurons provide trophic signal to the heart via β2-adrenoceptor-dependent regulation of proteolysis. *Cardiovasc Res*. 2013;97:240–250. doi: 10.1093/cvr/cvs320.
19. Zaglia T, Di Bona A, Chioato T, Basso C, Ausoni S, Mongillo M. Optimized protocol for immunostaining of experimental GFP-expressing and human hearts. *Histochem Cell Biol*. 2016;146:407–419. doi: 10.1007/s00418-016-1456-1.
20. Xiao DY, Luo S, O'Brian K, Liu W, Carson KR. Weight change trends and overall survival in United States veterans with follicular lymphoma treated with chemotherapy. *Leuk Lymphoma*. 2017;58:851–858. doi: 10.1080/10428194.2016.1217526.
21. Awad S, Tan BH, Cui H, Bhalla A, Fearon KC, Parsons SL, Catton JA, Lobo DN. Marked changes in body composition following neoadjuvant chemotherapy for oesophagogastric cancer. *Clin Nutr*. 2012;31:74–77. doi: 10.1016/j.clnu.2011.08.008.
22. Ghigo A, Li M, Hirsch E. New signal transduction paradigms in anthracycline-induced cardiotoxicity. *Biochim Biophys Acta*. 2016;1863(7 Pt B):1916–1925. doi: 10.1016/j.bbamcr.2016.01.021.
23. Yu X, Long YC, Shen HM. Differential regulatory functions of three classes of phosphatidylinositol and phosphoinositide 3-kinases in autophagy. *Autophagy*. 2015;11:1711–1728. doi: 10.1080/15548627.2015.1043076.
24. Nakai A, Yamaguchi O, Takeda T, Higuchi Y, Hikoso S, Taniike M, Omiya S, Mizote I, Matsumura Y, Asahi M, Nishida K, Hori M, Mizushima N, Otsu K. The role of autophagy in cardiomyocytes in the basal state and in response to hemodynamic stress. *Nat Med*. 2007;13:619–624. doi: 10.1038/nm1574.
25. Zaglia T, Milan G, Ruhs A, Franzoso M, Bertaggia E, Pianca N, Carpi A, Carullo P, Pesce P, Sacerdoti D, Sarais C, Catalucci D, Krüger M, Mongillo M, Sandri M. Atrogin-1 deficiency promotes cardiomyopathy and premature death via impaired autophagy. *J Clin Invest*. 2014;124:2410–2424. doi: 10.1172/JCI66339.
26. Li DL, Wang ZV, Ding G, Tan W, Luo X, Criollo A, Xie M, Jiang N, May H, Kyrychenko V, Schneider JW, Gillette TG, Hill JA. Doxorubicin blocks cardiomyocyte autophagic flux by inhibiting lysosome acidification. *Circulation*. 2016;133:1668–1687. doi: 10.1161/CIRCULATIONAHA.115.017443.
27. Bartlett JJ, Trivedi PC, Yeung P, Kienesberger PC, Pulinilkunnil T. Doxorubicin impairs cardiomyocyte viability by suppressing transcription factor EB expression and disrupting autophagy. *Biochem J*. 2016;473:3769–3789. doi: 10.1042/BCJ20160385.
28. Ikeda Y, Shirakabe A, Maejima Y, Zhai P, Sciarretta S, Toli J, Nomura M, Mihara K, Egashira K, Ohishi M, Abdellatif M, Sadoshima J. Endogenous Drp1 mediates mitochondrial autophagy and protects the heart against energy stress. *Circ Res*. 2015;116:264–278. doi: 10.1161/CIRCRESAHA.116.303356.
29. Hoshino A, Mita Y, Okawa Y, Ariyoshi M, Iwai-Kanai E, Ueyama T, Ikeda K, Ogata T, Matoba S. Cytosolic p53 inhibits Parkin-mediated mitophagy and promotes mitochondrial dysfunction in the mouse heart. *Nat Commun*. 2013;4:2308. doi: 10.1038/ncomms3308.
30. Luo L, Wall AA, Yeo JC, Condon ND, Norwood SJ, Schoenwaelder S, Chen KW, Jackson S, Jenkins BJ, Hartland EL, Schroder K, Collins BM, Sweet MJ, Stow JL. Rab8a interacts directly with PI3Kγ to modulate TLR4-driven PI3K and mTOR signalling. *Nat Commun*. 2014;5:4407. doi: 10.1038/ncomms5407.
31. Bohnacker T, Marone R, Collmann E, Calvez R, Hirsch E, Wymann MP. PI3Kγ adaptor subunits define coupling to degranulation and cell motility by distinct PtdIns(3,4,5)P3 pools in mast cells. *Sci Signal*. 2009;2:ra27–ra27. doi: 10.1126/scisignal.2000259.
32. De Leo MG, Staiano L, Vicinanza M, Luciani A, Carissimo A, Mutarelli M, Di Campli A, Polishchuk E, Di Tullio G, Morra V, Levtchenko E, Oltrabella F, Starborg T, Santoro M, Di Bernardo D, Devuyst O, Lowe M, Medina DL, Ballabio A, De Matteis MA. Autophagosome-lysosome fusion triggers a lysosomal response mediated by TLR9 and controlled by OCRL. *Nat Cell Biol*. 2016;18:839–850. doi: 10.1038/ncb3386.
33. Nazio F, Strappazzon F, Antonioli M, Bielli P, Cianfanelli V, Bordi M, Gretzmeier C, Dengjel J, Piacentini M, Fimia GM, Cecconi F. mTOR inhibits autophagy by controlling ULK1 ubiquitylation, self-association and function through AMBRA1 and TRAF6. *Nat Cell Biol*. 2013;15:406–416. doi: 10.1038/ncb2708.
34. Lamb CA, Yoshimori T, Tooze SA. The autophagosome: origins unknown, biogenesis complex. *Nat Rev Mol Cell Biol*. 2013;14:759–774. doi: 10.1038/nrm3696.
35. Stěrba M, Popelová O, Vávrová A, Jirkovský E, Kovaříková P, Geršl V, Simůnek T. Oxidative stress, redox signaling, and metal chelation in anthracycline cardiotoxicity and pharmacological cardioprotection. *Antioxid Redox Signal*. 2013;18:899–929. doi: 10.1089/ars.2012.4795.
36. Ali K, Soond DR, Pineiro R, Hagemann T, Pearce W, Lim EL, Bouabe H, Scudamore CL, Hancox T, Maecker H, Friedman L, Turner M, Okkenhaug K, Vanhaesebroeck B. Inactivation of PI(3)K p110δ breaks regulatory T-cell-mediated immune tolerance to cancer. *Nature*. 2014;510:407–411. doi: 10.1038/nature13444.
37. Mantovani A, Marchesi F, Malesci A, Laghi L, Allavena P. Tumour-associated macrophages as treatment targets in oncology. *Nat Rev Clin Oncol*. 2017;14:399–416. doi: 10.1038/nrclinonc.2016.217.
38. Mantovani A, Sozzani S, Locati M, Allavena P, Sica A. Macrophage polarization: tumor-associated macrophages as a paradigm for polarized M2 mononuclear phagocytes. *Trends Immunol*. 2002;23:549–555. doi: 10.1016/S1471-4906(02)02302-5.
39. Zhang S, Liu X, Bawa-Khalfe T, Lu LS, Lyu YL, Liu LF, Yeh ET. Identification of the molecular basis of doxorubicin-induced cardiotoxicity. *Nat Med*. 2012;18:1639–1642. doi: 10.1038/nm.2919.
40. Ichikawa Y, Ghanefar M, Bayeva M, Wu R, Khechaduri A, Naga Prasad SV, Mutharasan RK, Naik TJ, Ardehali H. Cardiotoxicity of doxorubicin is mediated through mitochondrial iron accumulation. *J Clin Invest*. 2014;124:617–630. doi: 10.1172/JCI72931.
41. Oudit GY, Crackower MA, Eriksson U, Sarao R, Kozieradzki I, Sasaki T, Irie-Sasaki J, Gidrewicz D, Rybin VO, Wada T, Steinberg SF, Backx PH, Penninger JM. Phosphoinositide 3-kinase gamma-deficient mice are protected from isoproterenol-induced heart failure. *Circulation*. 2003;108:2147–2152. doi: 10.1161/01.CIR.0000091403.62293.2B.
42. Siragusa M, Katare R, Meloni M, Damilano F, Hirsch E, Emanueli C, Madeddu P. Involvement of phosphoinositide 3-kinase gamma in angiogenesis and healing of experimental myocardial infarction in mice. *Circ Res*. 2010;106:757–768. doi: 10.1161/CIRCRESAHA.109.207449.
43. Bartlett JJ, Trivedi PC, Pulinilkunnil T. Autophagic dysregulation in doxorubicin cardiomyopathy. *J Mol Cell Cardiol*. 2017;104:1–8. doi: 10.1016/j.yjmcc.2017.01.007.
44. Koleini N, Kardami E, Koleini N, Kardami E. Autophagy and mitophagy in the context of doxorubicin-induced cardiotoxicity. *Oncotarget*. 2017;8:46663–46689. doi: 10.18632/oncotarget.16944.
45. Kawaguchi T, Takemura G, Kanamori H, Takeyama T, Watanabe T, Morishita K, Ogino A, Tsujimoto A, Goto K, Maruyama R, Kawasaki M, Mikami A, Fujiwara T, Fujiwara H, Minatoguchi S. Prior starvation mitigates acute doxorubicin cardiotoxicity through restoration of autophagy in affected cardiomyocytes. *Cardiovasc Res*. 2012;96:456–465. doi: 10.1093/cvr/cvs282.
46. Chen YR, Zweier JL. Cardiac mitochondria and reactive oxygen species generation. *Circ Res*. 2014;114:524–537. doi: 10.1161/CIRCRESAHA.114.300559.
47. Wymann MP, Zvelebil M, Laffargue M. Phosphoinositide 3-kinase signalling–which way to target? *Trends Pharmacol Sci*. 2003;24:366–376. doi: 10.1016/S0165-6147(03)00163-9.
48. Billingham ME, Mason JW, Bristow MR, Daniels JR. Anthracycline cardiomyopathy monitored by morphologic changes. *Cancer Treat Rep*. 1978;62:865–872.
49. Krischer JP, Epstein S, Cuthbertson DD, Goorin AM, Epstein ML, Lipshultz SE. Clinical cardiotoxicity following anthracycline treatment for childhood cancer: the Pediatric Oncology Group experience. *J Clin Oncol*. 1997;15:1544–1552. doi: 10.1200/JCO.1997.15.4.1544.
50. Rochette L, Guenancia C, Gudjoncik A, Hachet O, Zeller M, Cottin Y, Vergely C. Anthracyclines/trastuzumab: new aspects of cardiotoxicity and molecular mechanisms. *Trends Pharmacol Sci*. 2015;36:326–348. doi: 10.1016/j.tips.2015.03.005.
51. Evans CA, Liu T, Lescarbeau A, Nair SJ, Grenier L, Pradeilles JA, Glenadel Q, Tibbitts T, Rowley AM, DiNitto JP, Brophy EE, O'Hearn EL, Ali JA, Winkler DG, Goldstein SI, O'Hearn P, Martin CM, Hoyt JG, Soglia JR, Cheung C, Pink MM, Proctor JL, Palombella VJ, Tremblay MR, Castro AC. Discovery of a selective phosphoinositide-3-kinase (PI3K)-γ inhibitor (IPI-549) as an immuno-oncology clinical candidate. *ACS Med Chem Lett*. 2016;7:862–867. doi: 10.1021/acsmedchemlett.6b00238.